NBS REPORT
7682

DESIGN OF EXPERIMENTS FOR REMOTE MICROWAVE PROBING OF THE ATMOSPHERE

by

B. R. Bean, R. L. Abbott
and E. R. Westwater

NBS

U. S. DEPARTMENT OF COMMERCE
NATIONAL BUREAU OF STANDARDS
BOULDER LABORATORIES
Boulder, Colorado

THE NATIONAL BUREAU OF STANDARDS

Functions and Activities

The functions of the National Bureau of Standards are set forth in the Act of Congress, March 3, 1901, as amended by Congress in Public Law 619, 1950. These include the development and maintenance of the national standards of measurement and the provision of means and methods for making measurements consistent with these standards; the determination of physical constants and properties of materials; the development of methods and instruments for testing materials, devices, and structures; advisory services to government agencies on scientific and technical problems; invention and development of devices to serve special needs of the Government; and the development of standard practices, codes, and specifications. The work includes basic and applied research, development, engineering, instrumentation, testing, evaluation, calibration services, and various consultation and information services. Research projects are also performed for other government agencies when the work relates to and supplements the basic program of the Bureau or when the Bureau's unique competence is required. The scope of activities is suggested by the listing of divisions and sections on the inside of the back cover.

Publications

The results of the Bureau's research are published either in the Bureau's own series of publications or in the journals of professional and scientific societies. The Bureau publishes three periodicals available from the Government Printing Office: The Journal of Research, published in four separate sections, presents complete scientific and technical papers; the Technical News Bulletin presents summary and preliminary reports on work in progress; and the Central Radio Propagation Laboratory Ionospheric Predictions provides data for determining the best frequencies to use for radio communications throughout the world. There are also five series of nonperiodical publications: Monographs, Applied Mathematics Series, Handbooks, Miscellaneous Publications, and Technical Notes.

A complete listing of the Bureau's publications can be found in National Bureau of Standards Circular 460, Publications of the National Bureau of Standards, 1901 to June 1947 ($1.25), and the Supplement to National Bureau of Standards Circular 460, July 1947 to June 1957 ($1.50), and Miscellaneous Publication 240, July 1957 to June 1960 (includes Titles of Papers Published in Outside Journals 1950 to 1959) ($2.25); available from the Superintendent of Documents, Government Printing Office, Washington 25, D.C.

NATIONAL BUREAU OF STANDARDS REPORT

NBS PROJECT
8380-12-83489

April 30, 1963

NBS REPORT
7682

DESIGN OF EXPERIMENTS FOR REMOTE MICROWAVE PROBING OF THE ATMOSPHERE

by

B. R. Bean, R. L. Abbott
and E. R. Westwater

A Technical Report to U. S. Army Signal
Research and Development Laboratory
(MIPR R-61-3-SC-00-91)
Fort Monmouth, New Jersey

NBS

U. S. DEPARTMENT OF COMMERCE
NATIONAL BUREAU OF STANDARDS
BOULDER LABORATORIES
Boulder, Colorado

DESIGN OF EXPERIMENTS FOR REMOTE MICROWAVE PROBING OF THE ATMOSPHERE

by

B. R. Bean, R. L. Abbott,
and E. R. Westwater

1. Introduction

The purpose of this report is to summarize progress to date on studies of the feasibility of remotely probing the atmosphere at microwave frequencies to determine atmospheric ~~pressure~~ humidity and temperature structure. This will involve first summarizing the work to date on atmospheric absorption of radio waves and the thermal noise properties of the atmosphere. Analysis of computed values of thermal noise has indicated promising experimental procedures to be followed in actually determining atmospheric temperature and humidity structure.

2. Thermal Noise

All substances with temperatures above absolute zero emit thermal radiation. The distribution of this energy throughout the frequency spectrum is characteristic of the temperature of the source and of the constituent materials of the source itself. For our purposes, the source of radiation is the atmosphere; the frequency region is the microwave region from 10-50 kmc.

General laws of thermodynamics relate the absorption characteristics of a medium to those of emission. Good absorbers of radiation are also good emitters, and vice versa. In the microwave region, the atmosphere is a good emitter, as well as a strong absorber, of radiation. We may, therefore, describe quantitatively both emission and absorption by the same parameter, namely the absorption coefficient.

The emission characteristics of any real body at a fixed frequency may be compared to those of a black body at the same temperature.

In the microwave region the noise energy emitted by a black body is given by the Rayleigh-Jeans law

$$\psi(\nu) = 8\pi kT \left(\frac{\nu}{c} \right)^2 \tag{1}$$

where

$\psi(\nu)$ = emitted black body flux density per unit frequency,

ν = frequency,

T = absolute temperature, $^{\circ}$K,

c = the velocity of light, and

k = Boltzmann's constant (1.38044 x 16 ergs/ K°).

The emission per unit length along an actual ray path may now be expressed as

$$B(\nu) = \gamma(\nu)\psi(\nu) \tag{2}$$

where $\gamma(\nu)$ = absorption per unit length.

Remembering that the fraction of energy absorbed in a path length ds is given by the optical depth $d\tau$ (= $\gamma(\nu)$ ds), we may obtain the differential equation for transmission of radiation through the atmosphere:

$$\frac{dI(\nu)}{d\tau} = -I(\nu) + \psi(\nu) \tag{3}$$

where $I(\nu)$ is the flux density per unit frequency. The solution to this radiative transfer equation is

$$I(\nu) = \sum_m I_m(\nu)\, e^{-\int_s^{r_m} d\tau} + \int_s^{\infty} \psi(\nu)\, e^{-\int_s^{r} d\tau}\, d\tau \tag{4}$$

where the summation extends over all discrete noise sources which may be present, $I_m(\nu)$ is the unattenuated flux density transmitted from the mth discrete source located at position r_m, s is the point of reception of energy, and the other symbols have their previous meaning. It should be recognized that the above integrals extend over a ray path determined by the refractive properties of the medium and cannot be evaluated unless these refractive properties are known.

In analogy to the temperature dependence of the noise energy as given by the Rayleigh-Jeans law, we may, in the microwave region, relate the intensity of radiation received from a particular direction, $I(\nu)$, to an equivalent temperature, $T_m(\nu)$, by the following relation

$$\frac{I(\nu) = 8\pi k T_m(\nu)}{\lambda^2}, \tag{5}$$

or, from (4)

$$T_m(\nu) = \sum_m T_{m,s}(\nu)\, e^{-\int_s^{r_m} d\tau} + \int_s^{\infty} T(r)\, e^{-\int_s^{r} d\tau}\, d\tau \tag{6}$$

This equivalent temperature is called the thermal noise temperature.

It is apparent that the thermal noise temperature of the atmosphere as measured by an antenna, will depend explicitly upon antenna orientation and the frequency, and implicitly upon the atmospheric conditions along the ray path giving rise to absorption and emission of energy. It seems plausible, therefore, that one could exploit this dependence of thermal noise on atmospheric conditions as a probe of atmospheric structure.

Thermal noise is equally important in receiving communications since it represents the lowest possible noise level that can be attained by an antenna immersed in the atmosphere. This minimum noise level will, of course, vary, depending on atmospheric conditions, the frequency, and the antenna orientation.

3. Attenuation by Atmospheric Gases

It was pointed out in the previous section that the emission and absorption characteristics of the atmosphere can both be described by the absorption coefficient. Fortunately, for our purposes, gaseous absorption has previously drawn much attention, both theoretically and experimentally, and is fairly well understood.

The major atmospheric gases that need to be considered as absorbers in the frequency range of 100 to 50,000 Mc are water vapor and oxygen. For these frequencies the gaseous absorption rises principally in the 1.35 cm line (22,235 Mc) of water vapor and the series of lines centered around 0.5 cm (60,000 Mc) of oxygen [Van Vleck, 1947a, b]. The frequency dependence of these absorptions is shown in figure 1 [Van Vleck, 1947a].

In connection with figure 1, the water vapor absorption values have been adjusted to correspond to the mean absolute humidity, ρ , (grams of water vapor per cubic meter) for Washington, D. C., 7.75 g/m^3 The reason for this adjustment is that water vapor absorption is directly proportional to the absolute humidity [Van Vleck, 1951] and thus, variations in signal intensity due to water vapor absorption may be specified directly in terms of the variations in the absolute humidity of the atmosphere.

It can be seen from figure 1 that the water vapor absorption exceeds the oxygen absorption in the frequency range 13,000 Mc to 32,000 Mc, indicating that in this frequency range the total absorption will be the most sensitive to changes in the water vapor content of the air, while outside this frequency range the absorption will be more sensitive to changes in oxygen density. Only around the resonant frequency corresponding to λ = 1.35 cm is the water vapor absorption greater than the oxygen absorption. The absorption equations and the conditions under which they are applicable

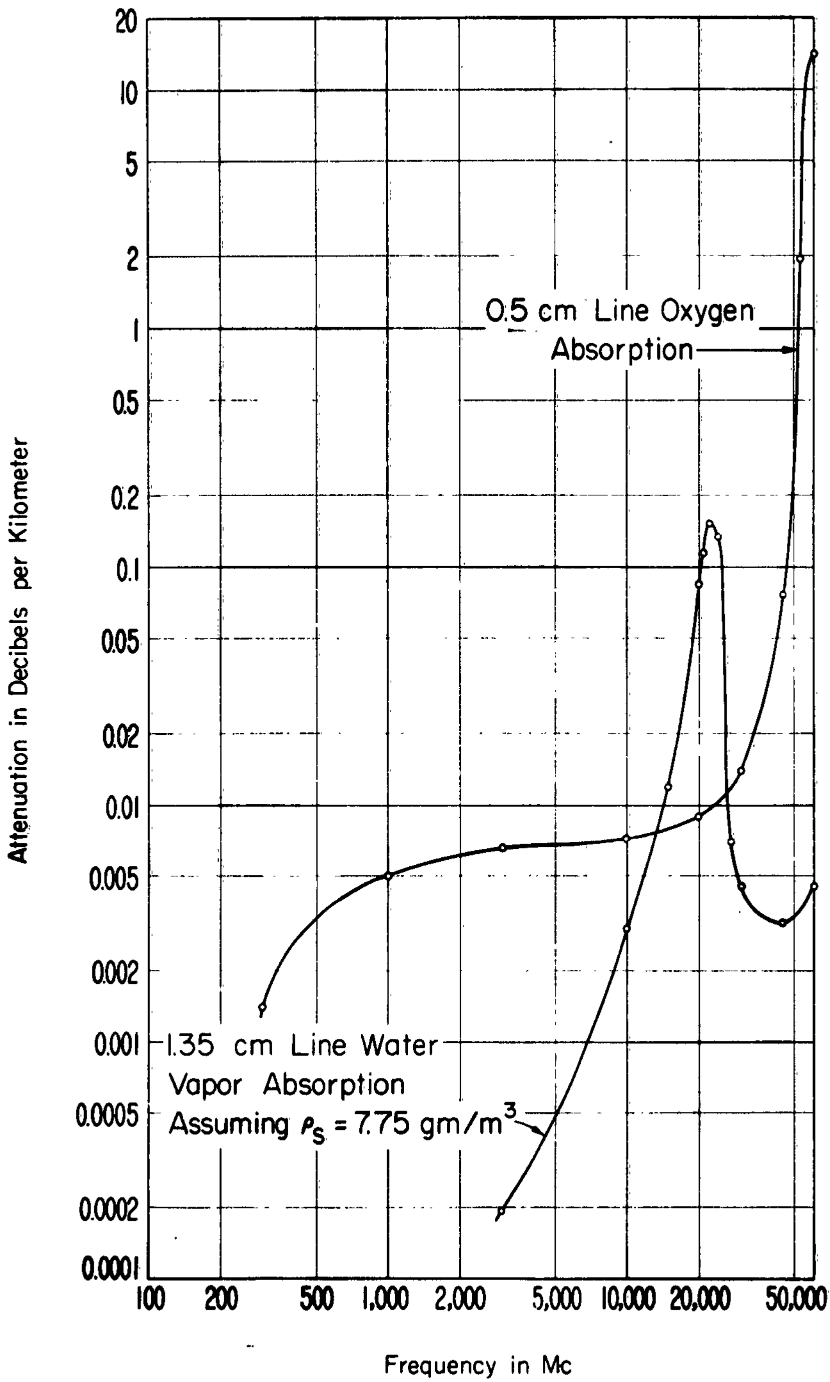

Fig. 1. Atmospheric absorption by the 1.35 cm line of water vapor and the 0.5 cm line of oxygen.

have been discussed by Van Vleck, [1947a].

The Van Vleck theory describes these absorptions in the following manner: the oxygen absorption at $T = 293^{\circ}K$ and atmospheric pressure in decibels per kilometer, γ_1, is given by the expression:

$$\gamma_1 = \frac{0.34}{\lambda^2}\left[\frac{\Delta\nu_1}{\frac{1}{\lambda^2} + \Delta\nu_1^2} + \frac{\Delta\nu_2}{\left(2 + \frac{1}{\lambda}\right)^2 + \Delta\nu_2^2} + \frac{\Delta\nu_2}{\left(2 - \frac{1}{\lambda}\right)^2 + \Delta\nu_2^2}\right] \quad (7)$$

where λ is the wave length for which the absorption is to be determined and where $\Delta\nu_1$ and $\Delta\nu_2$ are ½ line width factors with dimensions of cm^{-1}. This formula is based on the approximations of collision broadening theory. This theory postulates that, although the electromagnetic energy is freely exchanged between the incident field and the molecules, some of the electromagnetic energy is converted into thermal energy during molecular collisions and thus a part of the incident electromagnetic energy is absorbed. The term in (7) involving $\Delta\nu_1$ gives the nonresonant absorption arising from the zero frequency line of oxygen molecules while the terms involving $\Delta\nu_2$ describe the effects of the several natural resonant absorptions of the oxygen molecule which are in the vicinity of 0.5 cm wavelength. The $(2 \pm 1/\lambda)(cm^{-1})$ terms are the portion of the shape factors that describe the decay of the absorption at frequencies away from the resonant frequency (the number 2 is the reciprocal of the centroid resonant wavelength 0.5 cm).

The water vapor absorption at $293^{\circ}K$, rising from the 1.35 cm line. γ_2, is given by:

$$\frac{\gamma_2}{\rho} = \frac{3.5 \times 10^{-3}}{\lambda^2}\left[\frac{\Delta\nu_3}{\left(\frac{1}{\lambda} - \frac{1}{1.35}\right)^2 + \Delta\nu_3^2} + \frac{\Delta\nu_3}{\left(\frac{1}{\lambda} + \frac{1}{1.35}\right)^2 + \Delta\nu_3^2}\right] \quad (8)$$

where ρ is the absolute humidity and $\Delta\nu_3$ is the ½ line width factor of the 1.35 cm water vapor absorption line. The additional absorption arising from absorption bands above the 1.35 cm line, γ_3, is described by:

$$\frac{\gamma_3}{\rho} = \frac{.05\ \Delta\nu_4}{\lambda^2} \qquad (9)$$

where $\Delta\nu_4$ is the effective ½ line width of the absorption bands above the 1.35 cm line. The non-resonant term has been increased by a factor of 4 over the original Van Vleck formula in order to better satisfy experimental results. [Becker and Autler, 1946.]

Although Van Vleck gives estimates of the various line widths, more recent experimental determinations were used whenever possible. The line width values used in this paper are summarized in table 1.

Table 1: Line Width Factors Used to Determine Atmospheric Absorption

Line Width	Temperature	Value	Sources
$\Delta\nu_1$	293°K	0.018 cm^{-1} $atmosphere^{-1}$	Birnbaum & Maryott [1955]
$\Delta\nu_2$	300°K	0.049 cm^{-1} $atmosphere^{-1}$	J.O. Artman & J.P. Gordon [1953]
$\Delta\nu_3$	318°K	0.087 cm^{-1} $atmosphere^{-1}$	G.E. Becker & S.H. Autler [1946]
$\Delta\nu_4$	318°K	0.087 cm^{-1} $atmosphere^{-1}$	G.E. Becker & S.H. Autler [1946]

The preceding expressions for gâseous absorption are given as they appear in the literature and do not reflect the pressure and temperature sensitivity of either the numerical intensity factor or the line widths. This sensitivity must be considered for the present application since it is necessary to consider the manner in which the absorption varies with temperature and pressure variations throughout the atmosphere. The dependence of intensity factors upon atmospheric pressure and temperature variations was considered to be that given by the Van Vleck theory.

The magnitude and temperature dependence of the line widths is a question not completely resolved. Both theory and experiment indicate the line width to vary as $(1/T)^x$, $x > 0$. Different measurements on the same line of oxygen have given values of x ranging from .71 to .90 with differences in the magnitude of $\Delta\nu$ of about 20% [Tinkham and Strandberg, 1955; Hill and Gordy, 1954]. Experiments have also clearly indicated that the line width changes from line to line, with maximum fluctuations of about 15%. In the frequency region considered in this paper (10-45 kmc) the centroid frequency approximation for oxygen is valid and a mean line width can be used with good accuracy, but in the region of the resonant frequencies of oxygen, these line-to-line line width variations must be taken into account. The expressions used to calculate the absorptions are given in table 2. The reference temperatures given are those at which the appropriate experimental determinations were made, and the pressures are to be expressed in millibars. A detailed discussion of the theoretical aspects of the pressure and temperature dependence is given by Artman and Gordon [1953].

Experimental measurements on the absorption of microwaves by the atmosphere, (performed after our original work), show different values of the loss than those obtained by theoretical prediction methods. There is reasonably good agreement between the predicted and measured loss for oxygen, but the measured loss for water vapor is considerably greater than that of the predicted amount, particularly above 50,000 kmc [Straiton and Tolbert, 1960]. These observed discrepancies have little effect upon the present study, which is confined to frequencies less than 50 kmc. The results of the present study, for the frequency range 100 Mc-50,000 Mc, agree with those reached by Tolbert and Straiton [1957] in their field experiments at Cheyenne Mountain and Pikes Peak, Colorado, at altitudes of 14,000 feet.

Table 2. Values used in the Calculation of Atmospheric Absorption

Absorption [db/km]	Intensity Factor	Line Width
γ_1	$\frac{.34}{\lambda^2}\left(\frac{P}{1013.25}\right)\left(\frac{293}{T}\right)^2$	$\Delta\nu_1\left(\frac{P}{1013.25}\right)\left(\frac{293}{T}\right)^{3/4}$ and $\Delta\nu_2\left(\frac{P}{1013.25}\right)\left(\frac{300}{T}\right)^{3/4}$
$\frac{\gamma_2}{\rho}$*	$\frac{.0318}{\lambda^2}\left(\frac{293}{T}\right)^{5/2} e^{\frac{-644}{T}}$	$\Delta\nu_3\left(\frac{P}{1013.25}\right)\left(\frac{318}{T}\right)^{1/2}\left(1+.0046\rho\right)$
$\frac{\gamma_3}{\rho}$*	$\frac{.05}{\lambda^2}\left(\frac{293}{T}\right)$	$\Delta\nu_4\left(\frac{P}{1013.25}\right)\left(\frac{318}{T}\right)^{1/2}\left(1+.0046\rho\right)$

* ρ is water vapor density in gm/m^3.

The above approach represents that presented by Bean and Abbott in 1957. The following treatment was given by Gunn-East [1954] and based on Van Vleck's two papers [1947a, b]. This latter presentation is only valid when single line absorption with no appreciable overlap from adjacent lines is considered.

By taking into account the temperature and pressure dependence of the line widths it is seen that for a given quantity of water vapor, the attenuation is proportional to P^{-1} and $T^{-2} e^{-\frac{644}{T}}$ at the resonance line, to P and $T^{-3} e^{-\frac{644}{T}}$ at the sides of the curve and to P and $T^{-3/2}$ well away from resonance. In applying the above considerations to absorption approximations, it must also be kept in mind that for a given relative humidity, the density will vary considerably with temperature. Table 3 shows attenuation by water vapor at various temperatures and wavelengths. The behavior of water vapor attenuation near the resonant line is very remarkable, as may be seen by inspecting equation (8). Since $\Delta\nu_3$ is small compared to $\frac{1}{\lambda}$, for order of magnitude purposes it may be neglected in the denominator for non-resonant wavelengths. The attenuation per unit density is thus directly proportional to $\Delta\nu_3$ and hence to the total pressure for these frequencies. But at the resonant frequency, the dominant term in the expression is proportional to $\frac{1}{\Delta\nu_3}$ and thus inversely proportional to the pressure. In the atmosphere, the water vapor density is proportional to the total pressure. Therefore, the attenuation is independent of pressure at the resonant frequency and now depends only on the fraction of water vapor present. For practical purposes, this means that attenuation can occur at high altitudes with the same effectiveness as in the lower, denser layers if the mixing ratio is the same.

On the other hand, oxygen absorption occurs because of a large number of lines around 60 kMc. In the region from 3 to 45 kmc the attenuation is proportional to p^2 and to $T^{-5/2}$ [Gunn and East, 1954]. As the temperature decreases the attenuation increases gradually. At -40°C oxygen attenuation is about 78% higher than at 20°C due to increased density at low temperatures. Table 4 shows the pressure and temperature corrections for oxygen attenuation at the wavelengths between 0.7 and 10 cm.

Figure 2 shows the attenuation measured by Becker and Autler [1946]. The dashed line shows values calculated from Van Vleck's theory. The water vapor absorption curve, c, corresponds to a water content of 1 gm/m^3.

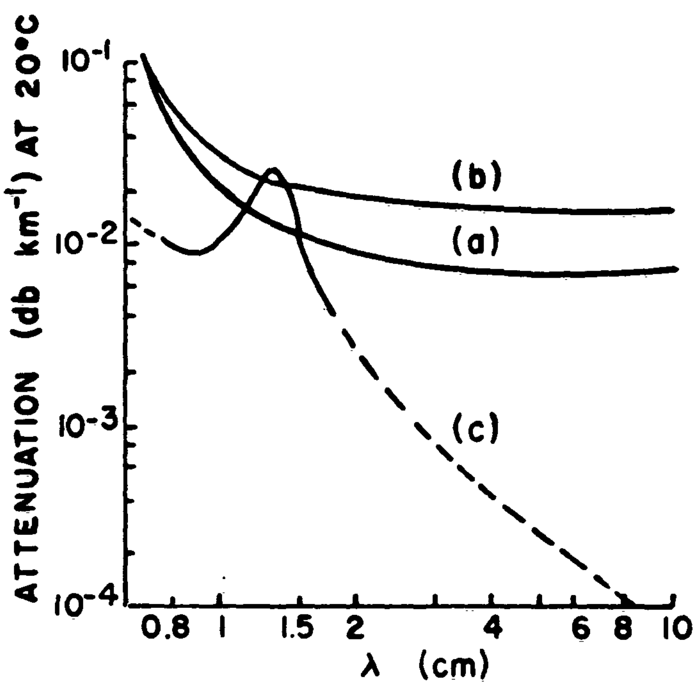

Fig. 2. Attenuation of microwaves by atmospheric gases. [Gunn and East]

Table 3

Water Vapor Attenuation (One way) in db/km [After Gunn-East]

P, pressure in atmospheres; W, water vapor content in g/m^{-3}

T(°C) λ(cm)	10	5.7	3.2	1.8	1.24	0.9
20	$0.07 \times 10^{-3} PW$	$0.24 \times 10^{-3} PW$	$0.7 \times 10^{-3} PW$	$4.3 \times 10^{-3} PW^*$	$22.0 \times 10^{-3} p^{-1} PW^*$	$9.5 \times 10^{-3} PW$
0	$0.08 \times 10^{-3} PW$	$0.27 \times 10^{-3} PW$	$0.8 \times 10^{-3} PW$	$4.8 \times 10^{-3} PW^*$	$23.3 \times 10^{-3} p^{-1} PW^*$	$10.4 \times 10^{-3} PW$
-20	$0.09 \times 10^{-3} PW$	$0.30 \times 10^{-3} PW$	$0.9 \times 10^{-3} PW$	$5.0 \times 10^{-3} PW^*$	$24.6 \times 10^{-3} p^{-1} PW^*$	$11.4 \times 10^{-3} PW$
-40	$0.10 \times 10^{-3} PW$	$0.34 \times 10^{-3} PW$	$1.0 \times 10^{-3} PW$	$5.4 \times 10^{-3} PW^*$	$26.1 \times 10^{-3} p^{-1} PW^*$	$12.6 \times 10^{-3} PW$

* The pressure dependencies shown are only approximate. Near 1.35 cm water vapor absorption line (between 1.0 cm and 2.0 cm) no simple power is accurate.

Table 4

Pressure and Temperature Correction for Oxygen Attenuation for Wavelengths between 0.7 and 10 cm [After Gunn-East]

T(°C)	Factor (P is pressure in atmospheres)
20	$1.00 P^2$
0	$1.19 P^2$
-20	$1.45 P^2$
-40	$1.78 P^2$

Since absorption is so sensitive to the absolute humidity level, it is helpful to have information on the climatic variations of absolute humidity throughout the 1 to 99% range of values normally used in radio engineering. Estimates of the values of absolute humidity at the surface expected 50% of the time for the United States for February and August are given in figures 3 and 4 respectively [Bean and Cahoon, 1957]. It is evident that for either month the coastal regions display greater values of absolute humidity than do the inland regions. Note that for any location the August values are consistently greater than the February values. Figures 5 to 8 show the values of absolute humidity expected to be exceeded 1 to 99% of the time throughout the United States in both summer and winter.

In addition to oxygen and water vapor, there are a number of other atmospheric gases which have absorption lines in the microwave region from 10 to 50 kmc. These gases normally constitute a negligible portion of the general composition of the atmosphere, but could conceivably contribute to attenuation. Table 5 shows the resonant frequencies, ν_o, maximum absorption coefficients at 300°K, α_{max}, (attenuation coefficient if the fraction of molecules present were equal to unity), expected concentration in the atmosphere and expected absorption coefficients, α, due to these trace constituents. The data on molecular absorption coefficients were taken from Ghosh and Edwards [1956], that on concentrations from the Compendium of Meteorology [1951]. It is readily seen that the attenuation due to these sources is negligible compared to the high absorption due to oxygen and water vapor.

4. Estimates of the Range of Total Gaseous Absorption

The range in gaseous absorption can be seen by considering the data for the months of February and August at Bismarck, North Dakota, and Washington, D. C., two stations with very different climates. The values of total gaseous absorption (defined as the sum of γ_1, γ_2, and γ_3,

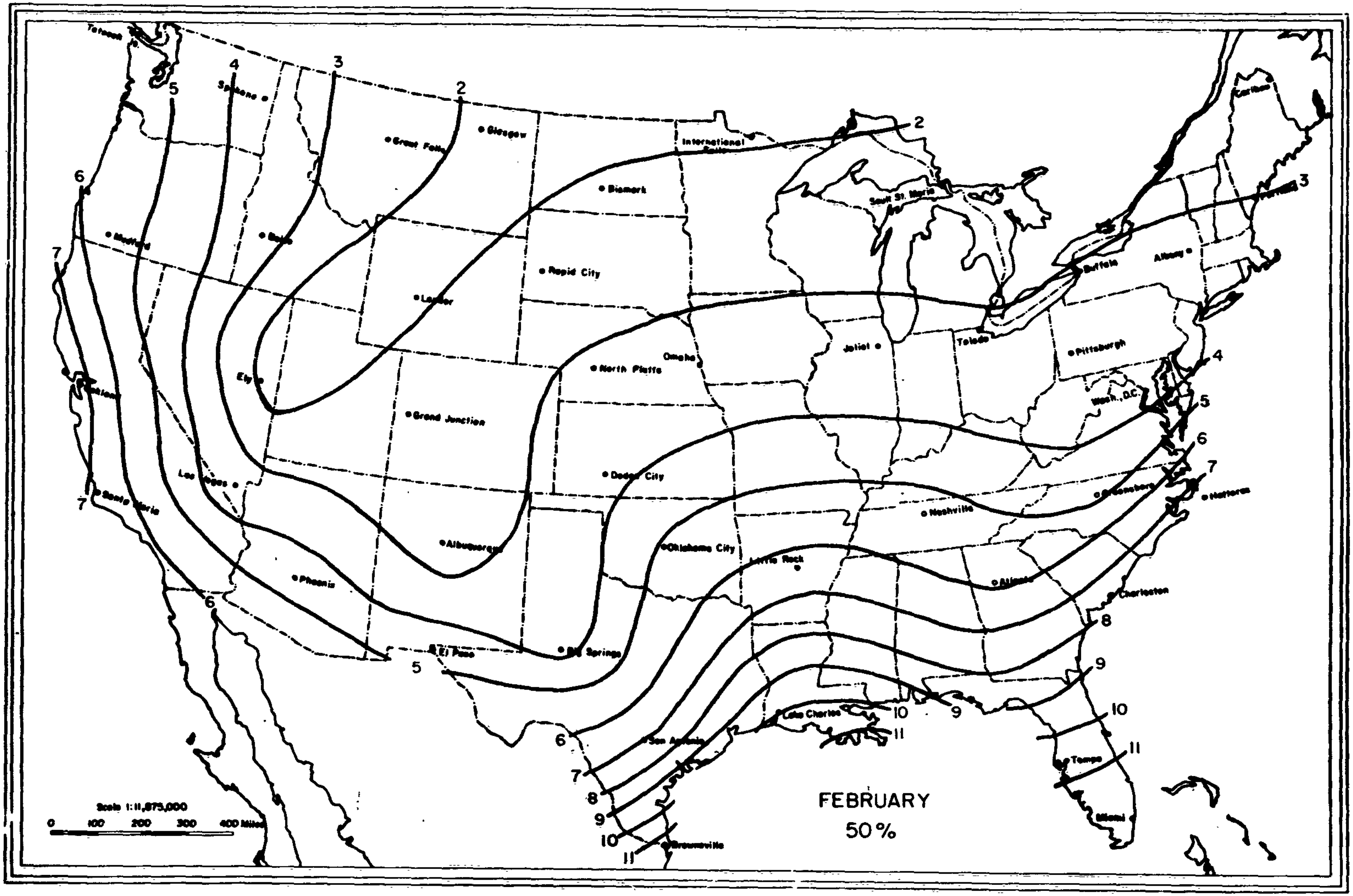

Fig. 3. Estimate of the value of absolute humidity expected 50 percent of the time for February.

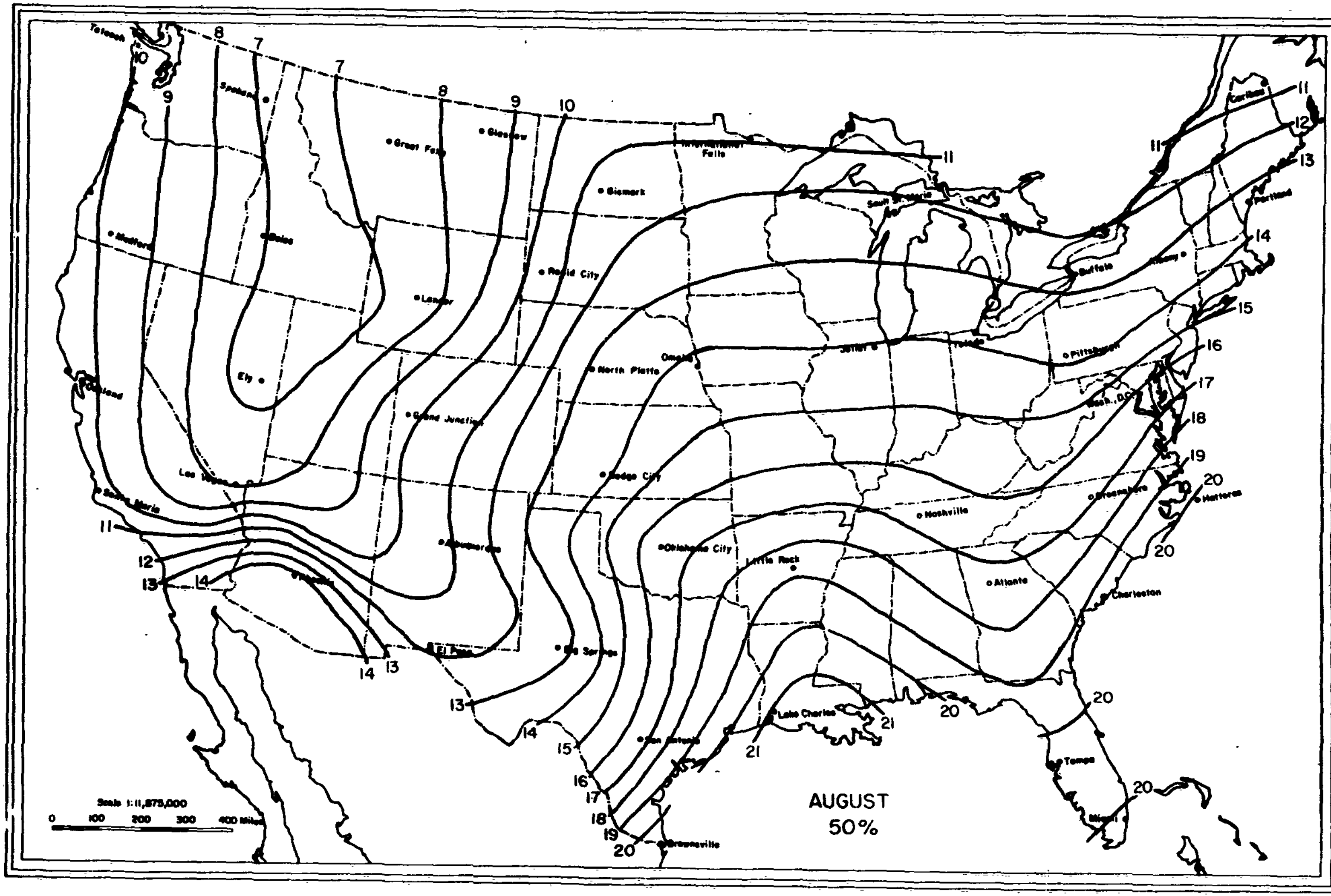

Fig. 4. Estimate of the value of absolute humidity expected 50 percent of the time for August.

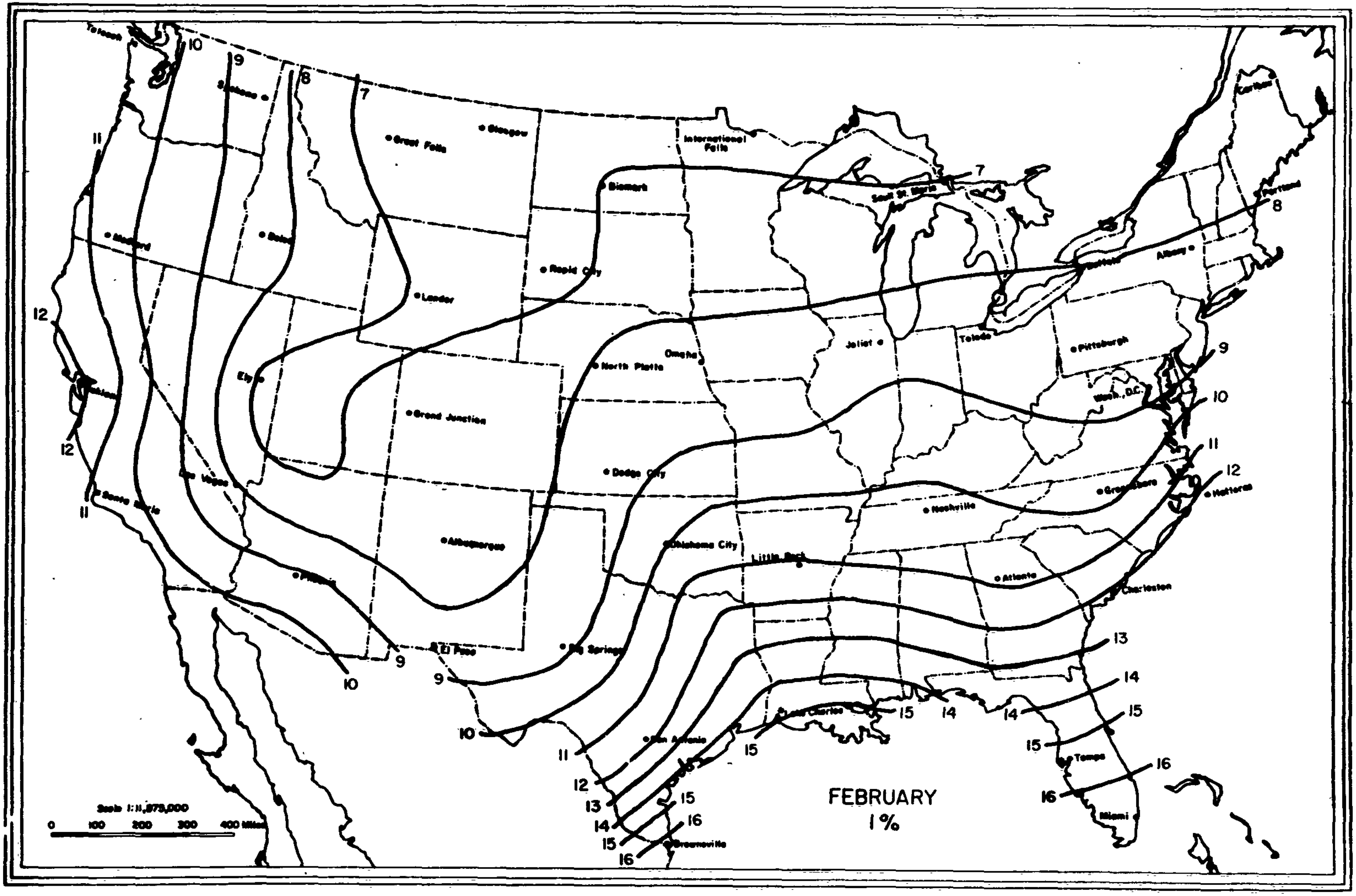

Fig. 5. Values of absolute humidity expected to be exceeded 1 percent of the time for February.

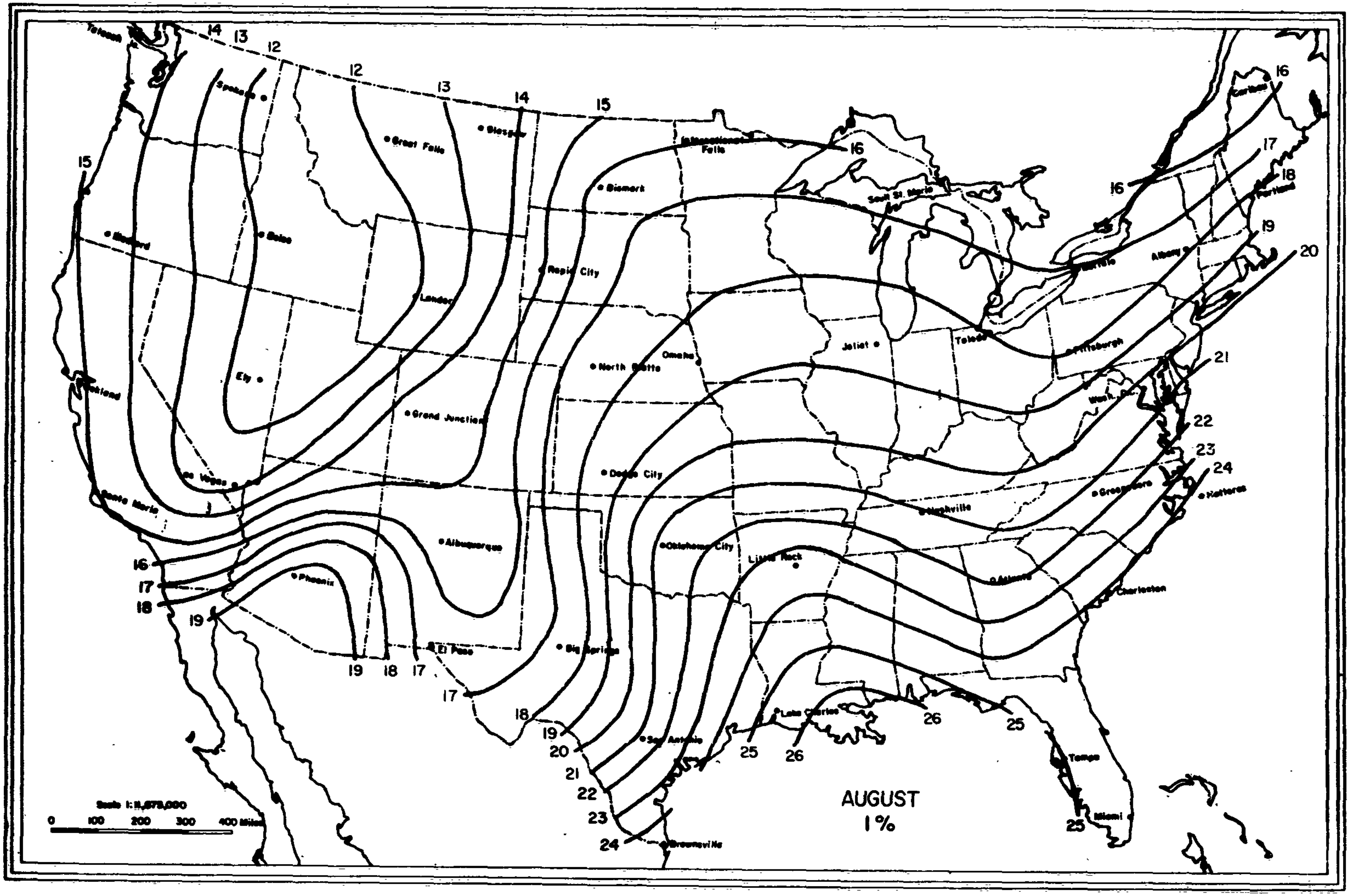

Fig. 6. Values of absolute humidity expected to be exceeded 1 percent of the time for August.

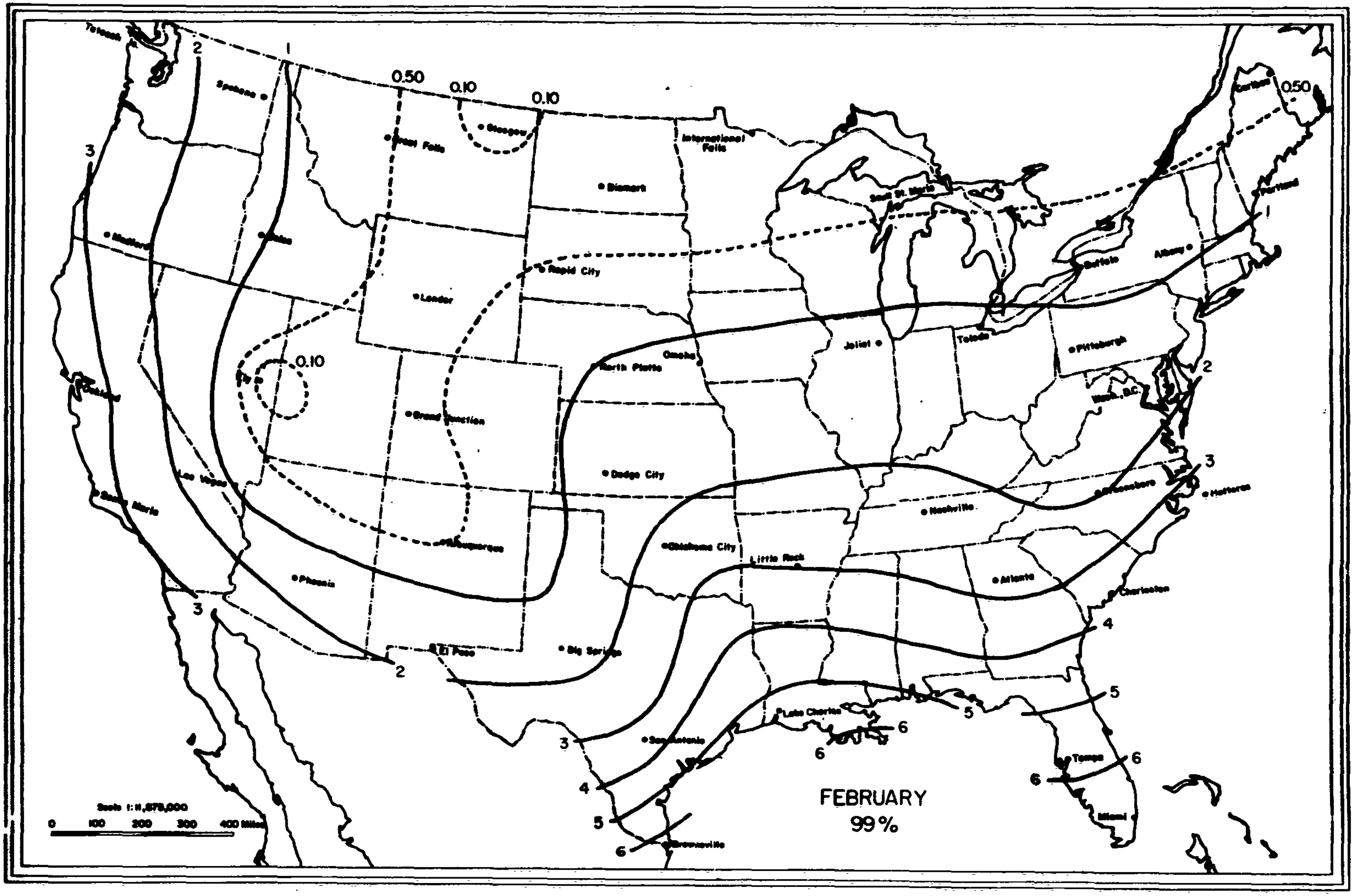

Fig. 7. Values of absolute humidity expected to be exceeded 99 percent of the time for February.

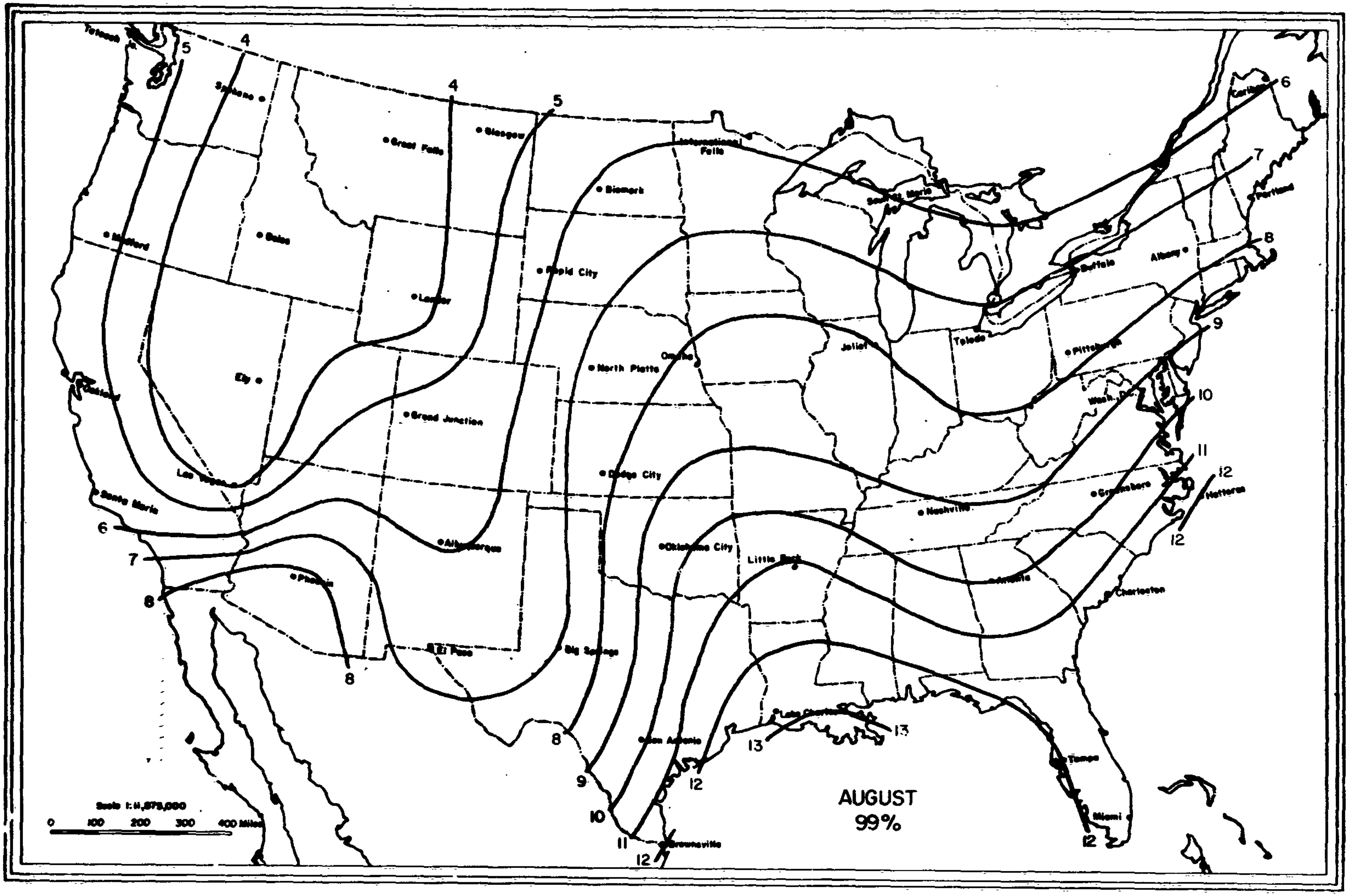

Fig. 8. Values of absolute humidity expected to be exceeded 99 percent of the time for August.

Table 5

Absorption Coefficients of Minor Atmospheric Gases

Gas	ν_o(Mc)	a_{max}(db/km)	% by volume at ground	a(db/km) at ground
SO_2	12,258.17	1.9×10^{-1}	$(0 \text{ to } 1)\times10^{-6}$	$(0-1.9)\times10^{-7}$
	12,854.54	8.7×10^{-1}		$(0-8.7)\times10^{-7}$
	23,433.42	1.2×10^{-1}		$(0-1.2)\times10^{-7}$
	24,304.96	2.3		$(0-2.3)\times10^{-6}$
	25,398.22	2.1		$(0-2.1)\times10^{-6}$
	29,320.36	3.3		$(0-3.3)\times10^{-6}$
	44,098.62	5.2		$(0-5.2)\times10^{-6}$
	52,030.60	9.5×10^{-1}		$(0-9.5)\times10^{-7}$
N_2O	24,274.78	2.5	0.5×10^{-6}	1.25×10^{-6}
	22,274.60	2.5		1.25×10^{-6}
	25,212.55	2.5		1.25×10^{-6}
	25,123.25	2.5		1.25×10^{-6}
NO_2	26,289.6	2.9	$(0 \text{ to } 2)\times10^{-8}$	$6 \text{ to } 5.8)\times10^{-8}$
O_3	10,247.3	9.5×10^{-2}	summer $(0 \text{ to } .07)\times10^{-6}$	$(0 \text{ to } 6.3)\times10^{-9}$
	11,075.9	9.1×10^{-2}	winter $(0 \text{ to } .02)\times10^{-6}$	$(0 \text{ to } 6.3)\times10^{-9}$
	42,832.7	4.3×10^{-1}		$(0 \text{ to } 2.8)\times10^{-8}$

where γ_1 = oxygen absorption in decibels per kilometer, γ_2 = water vapor absorption rising from the 1.35 cm line and γ_3 = additional absorption rising from absorption lines whose frequencies are considerably higher than that corresponsing to the 1.35 line) at each station and elevation up to 75,000 feet are shown in figures 9 and 10 for each of the four station months for the frequency range of 100 Mc to 50,000 Mc. Above 75,000 feet the absorption values for all four station months are identical and are given for each frequency in figure 11. The absolute humidity was calculated using the upper air monthly average values of temperature, pressure, and humidity as reported by Ratner [1945]. Readings for the relative humidity are not generally given in this report for altitudes greater than about 15 kilometers due to the inability of the radiosonde to measure the small amount of humidity present at these altitudes. It is believed that the climates represented by these station months encompass the range of those of the majority of the continental United States radio propagation paths.

An interesting property of the annual range of absorption as a function of the frequency may be seen in figures 9 and 10. For the first 5,000 feet above the surface, it is noted that in the frequency range of 10 to 32.5 kMc the summer values are greater than the winter values due to increased humidity of the summer months. Outside of this frequency range, however, the winter values of absorption are greater due to the increased oxygen density. The relevant parameter in ray tracing is the refractivity N($N = (n-1)x10^6$, where n is the refractive index). Equation (10) shows how N is related to the atmospheric parameters, pressure P (mb), temperature T (k^o), saturation vapor pressure e_s(mb) and relative humidity R:

$$N = \frac{77.6}{T}\left(P + \frac{4810\, e_s R}{T} \right) . \qquad (10)$$

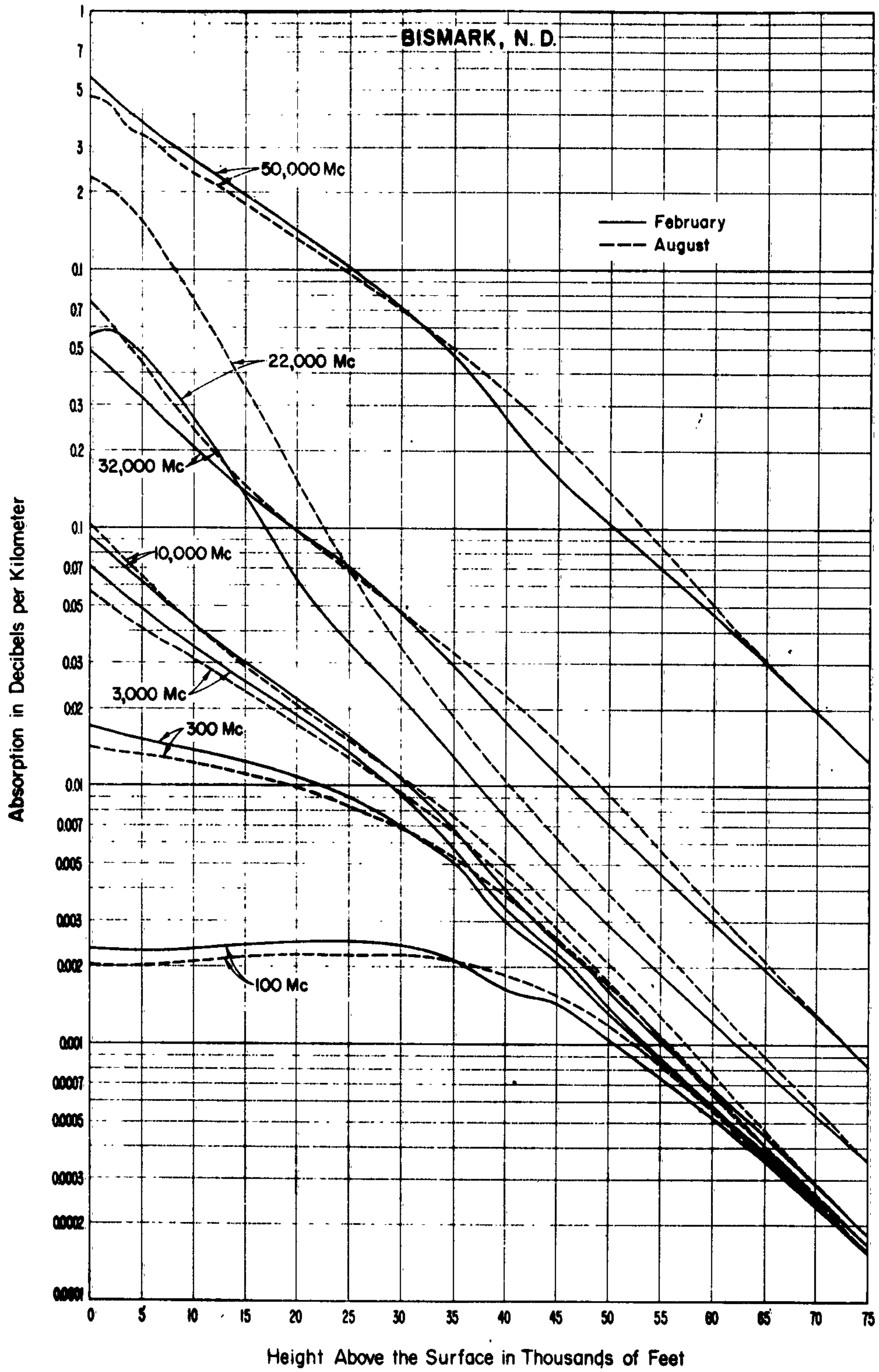

Fig. 9. Total gaseous atmospheric absorption fromthe surface to 75,000 feet: Bismarck, N. D.

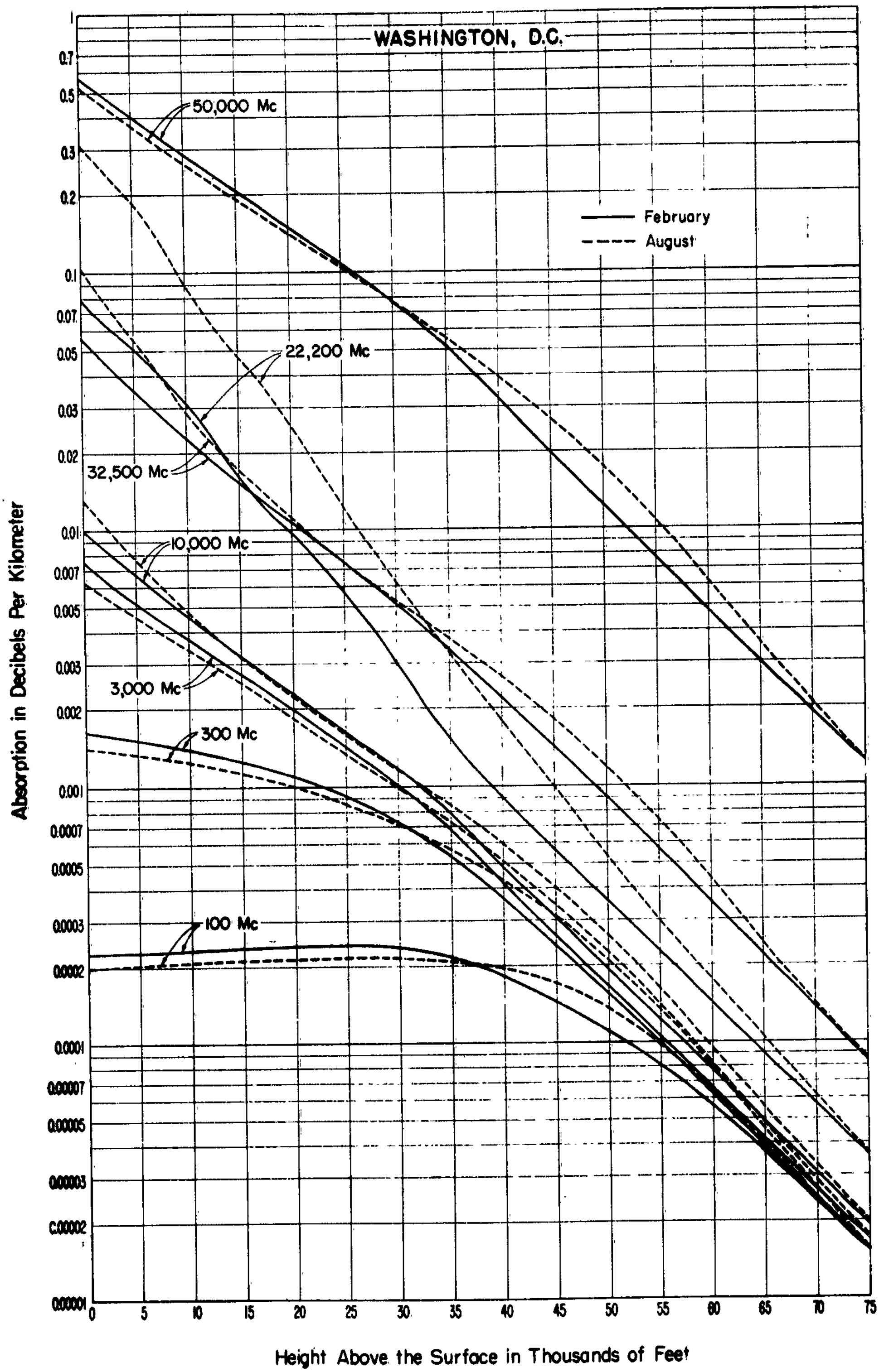

Fig. 10. Total gaseous atmospheric absorption from the surface to 75,000 feet: Washington, D. C.

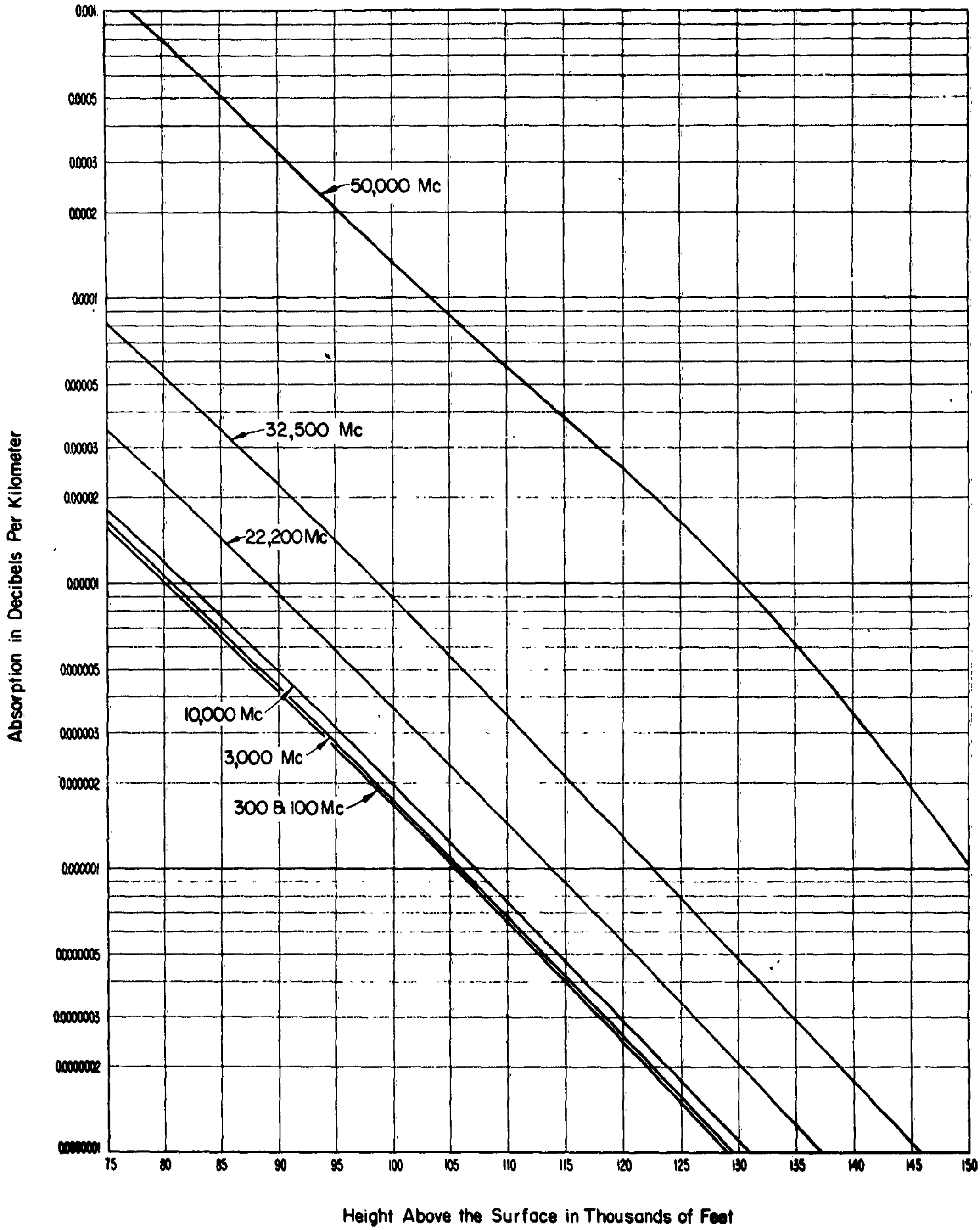

Fig. 11. Common values of total gaseous atmospheric absorption for elevations greater than 75,000 feet.

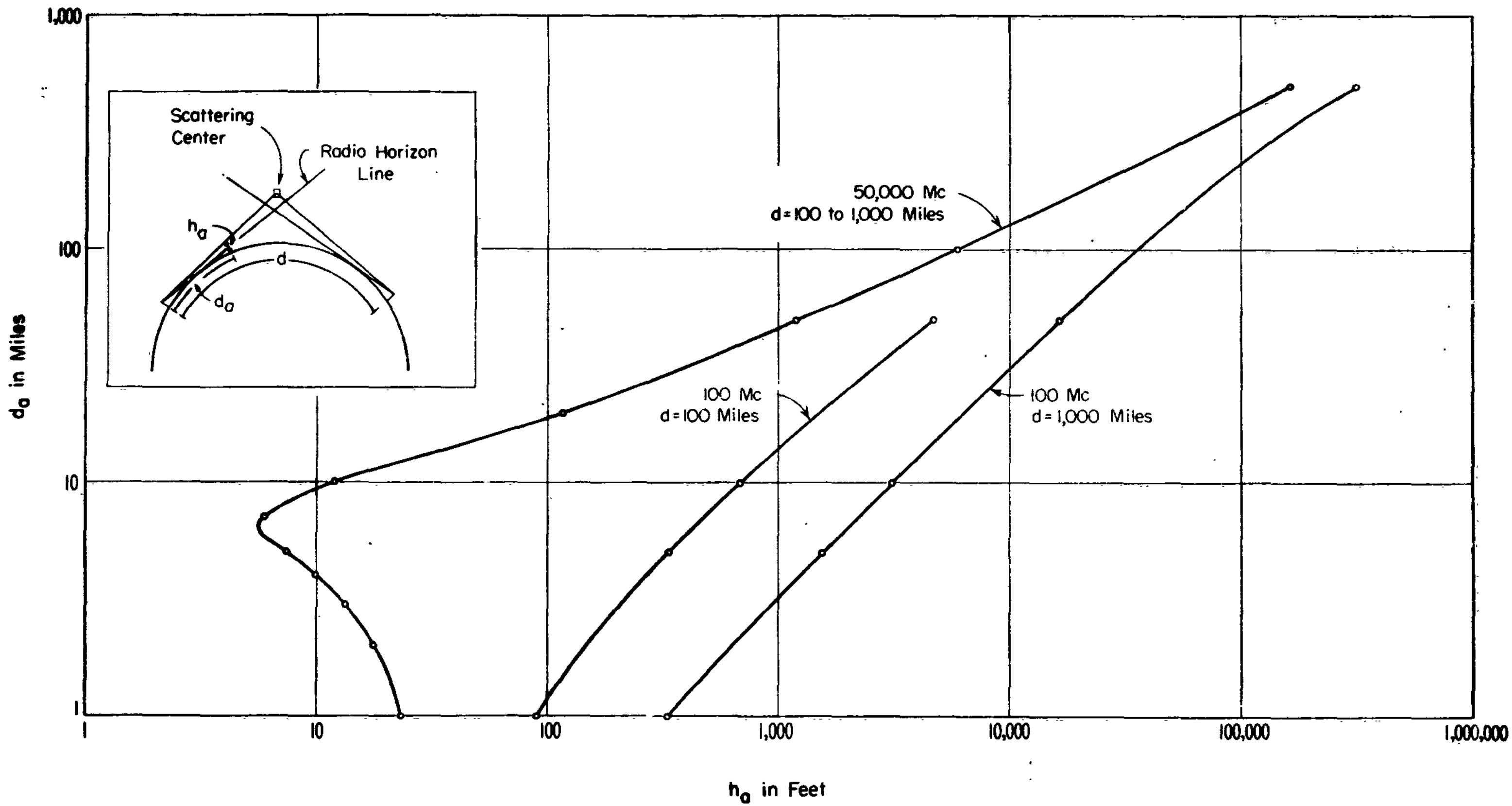

Fig. 12. Distance, d_a, along the radio ray to the scattering center versus the height, h_a, of the radio ray.

6. Design of Experiments

Thermal noise temperatures are subject to wide fluctuations on a geographical, seasonal, and diurnal basis. The mean thermal noise may be expected to be dependent on the altitude of the observing station through the pressure and mean surface temperature. The surface temperature effect is not as strong in the mean effect as the pressure since these are strong solar surface effects. On a diurnal basis the higher stations would be expected to show greater fluctuations.

One expects that the thermal noise temperature would be strongly dependent upon the angle of arrival of the radio ray. Rays incident at the receiving antenna near the horizontal sample a larger section of the lower atmosphere than vertical rays. In a normal atmosphere, rays incident from a horizontal direction traverse about 125 km to reach an altitude of 1 km, while of course, vertical rays traverse only 1 km. Horizontal rays are also very sensitive to the refractive index profile in this lowest portion of the atmosphere. Thus one would surmise that the thermal noise temperature is most sensitive to the detailed structure of the atmosphere when small angles of elevation are involved.

Thermal noise is also very dependent on the absolute humidity.

Vertical thermal noise measurements on the 1.33 cm line sample the total water vapor distribution and thus are an index of the total precipitable water above the station. When combined with information at other frequencies and angles it should yield significant information about the state of the lower atmosphere.

It seems clear that the use of the thermal noise temperature as a criterion for the temperature and water vapor profile of the atmosphere must involve both angle and frequency diversity. For the avoidance of competing sources it would seem that the best frequencies are those from about 8 to 38 kmc.

Analysis of our previously reported data indicates the probable direction of our continuing work upon developing a method of passive probing of the atmosphere at microwave frequencies.

Consider figures 13 to 16 where the thermal noise at water vapor resonance (λ = 1.339 cm), just off water vapor resonance (λ = 1.429 cm) and well off resonance (λ = 3 cm) are plotted versus angle of arrival of a radio ray at the earth's surface. The temperature and absolute humidity distributions with height for each of the four observations are given on figures 17 to 20. It is observed that the four cases shown are widely different in their atmospheric structure.

The dependence of thermal noise upon temperature and humidity structure is further emphasized by taking the difference between each case and the zero humidity standard atmosphere as previously reported. These differences, for each wavelength are given on figures 21 to 24.

It is observed that the curves given show differences in intercept, slope, position, and intensity of maximum, thus confirming the direction of the experimental program towards frequency and angular diversity measurements. It is evident that a model atmosphere may be selected that will emphasize the departures from standard more dramatically than the present choice. The work to be carried out under the continuation of this contract will thus seek to interpret the calculated values of thermal noise referenced to various standard atmospheres, taking full account of the fact that the initial values of temperature and humidity would in practice, be known.

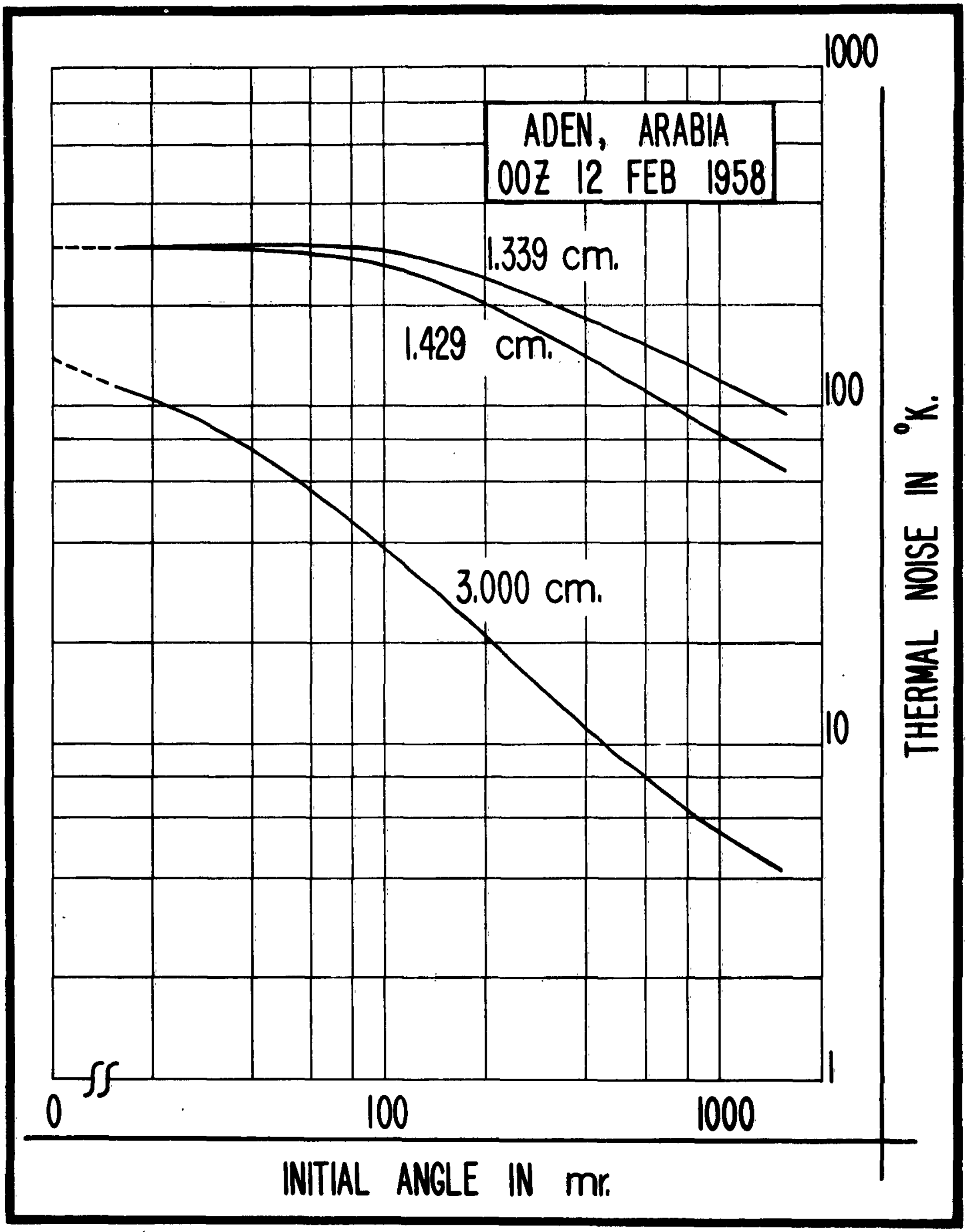

Fig. 13. Thermal noise temperature vs antenna elevation angle for several wavelengths at Aden, Arabia.

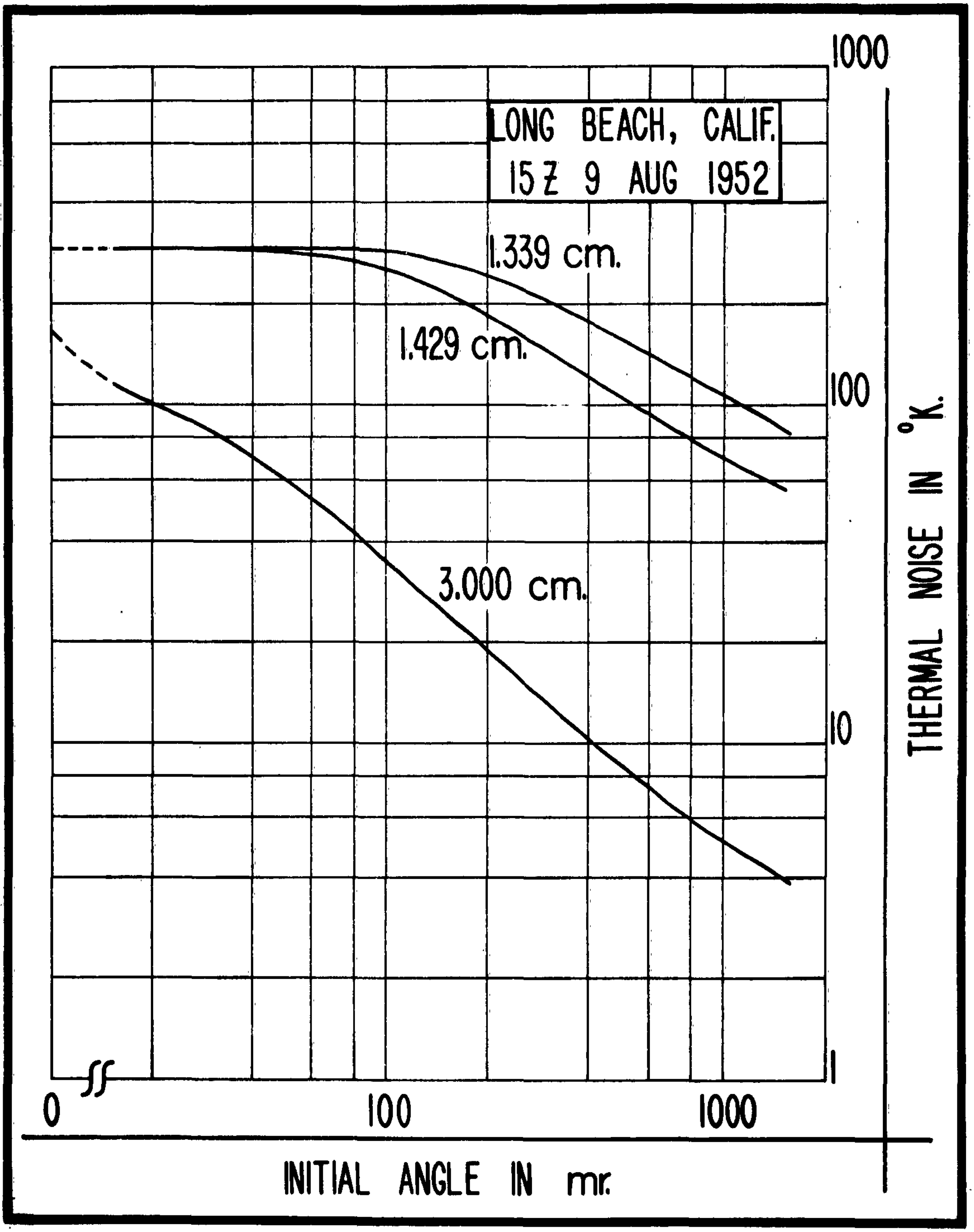

Fig. 14. Thermal noise temperature vs antenna elevation angle for several wavelengths at Long Beanch, California.

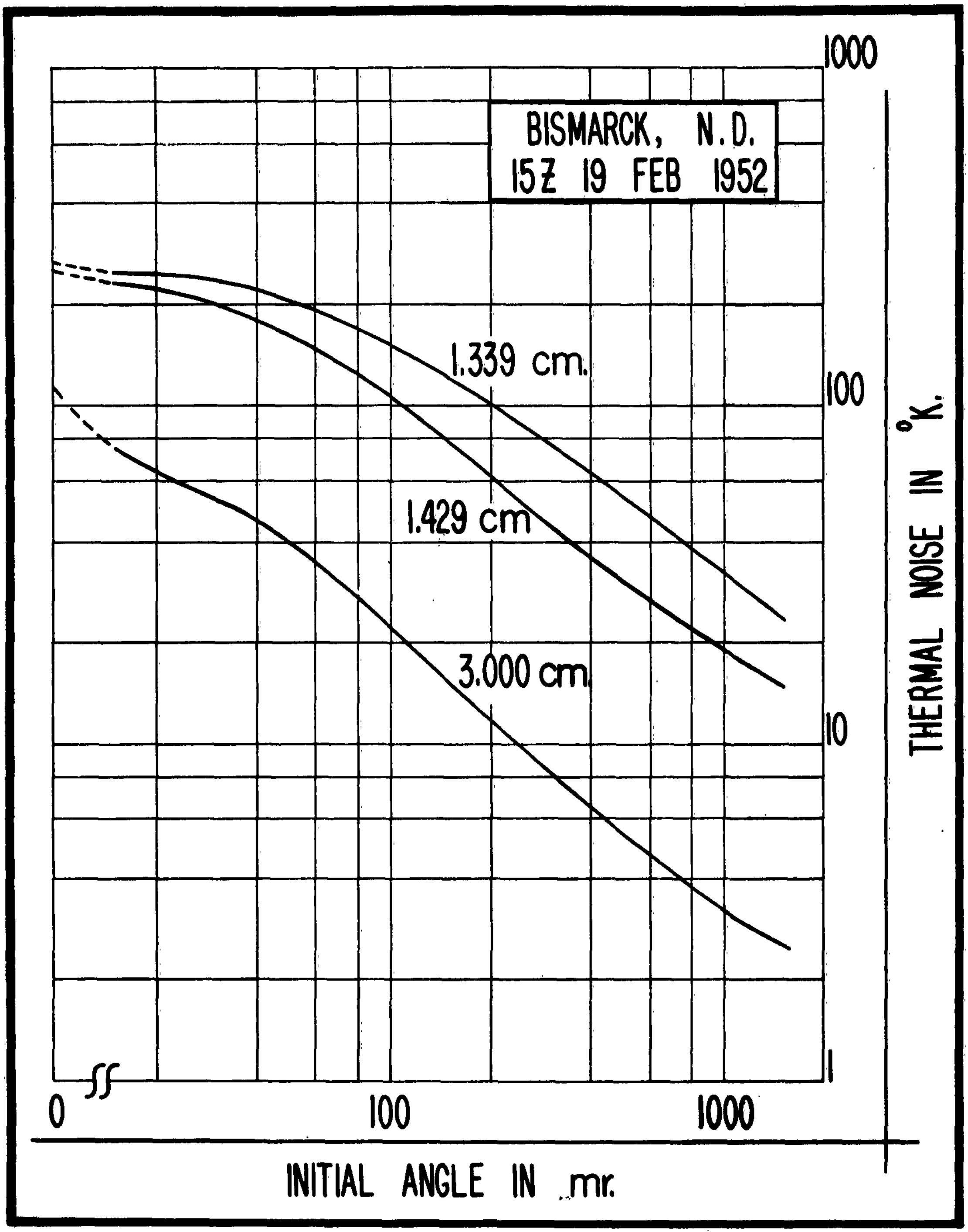

Fig. 15. Thermal noise temperature vs antenna elevation angle for several wavelengths at Bismarck, N. Dakota.

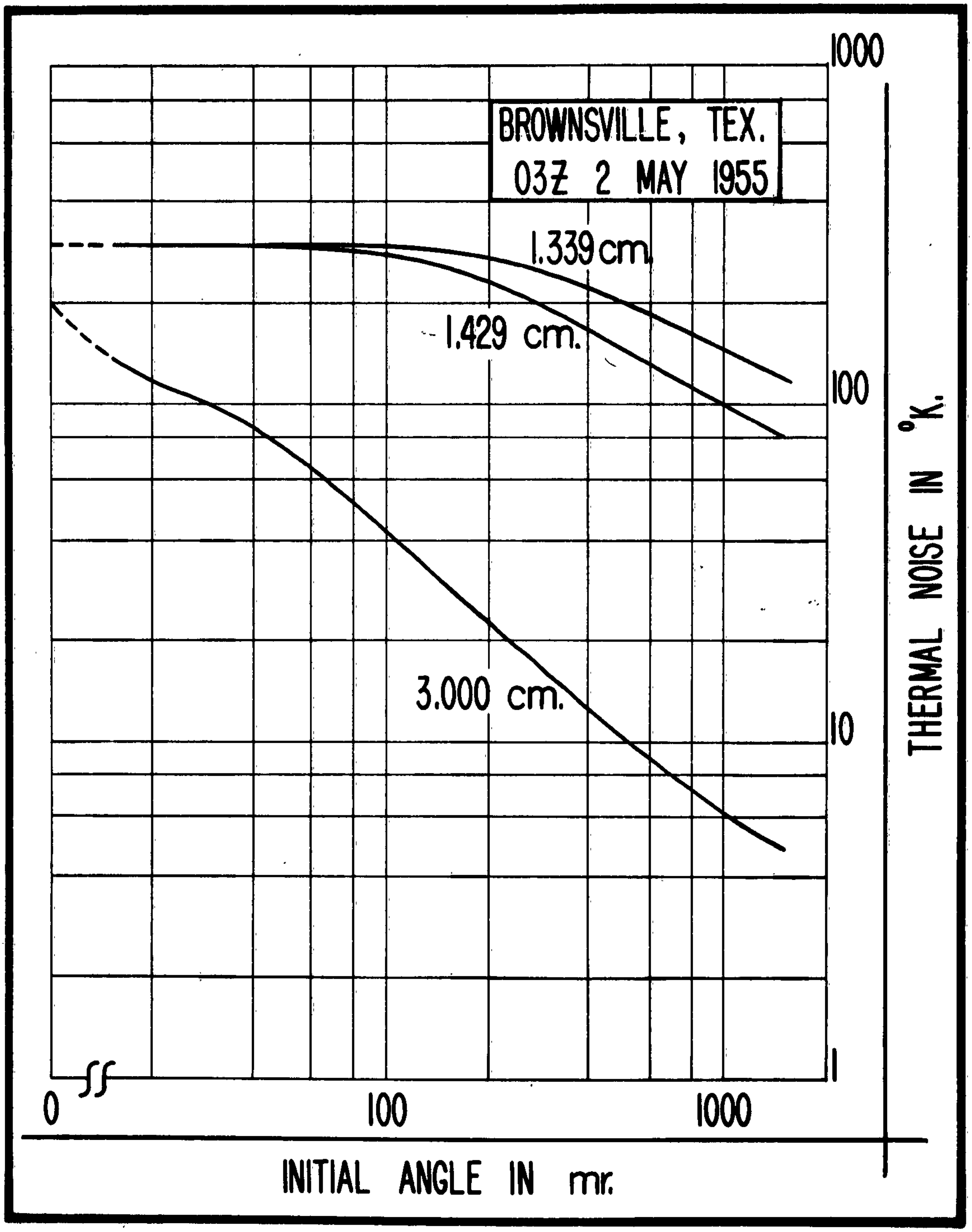

Fig. 16. Thermal noise temperature vs antenna elevation angle for several wavelengths at Brownsville, Texas.

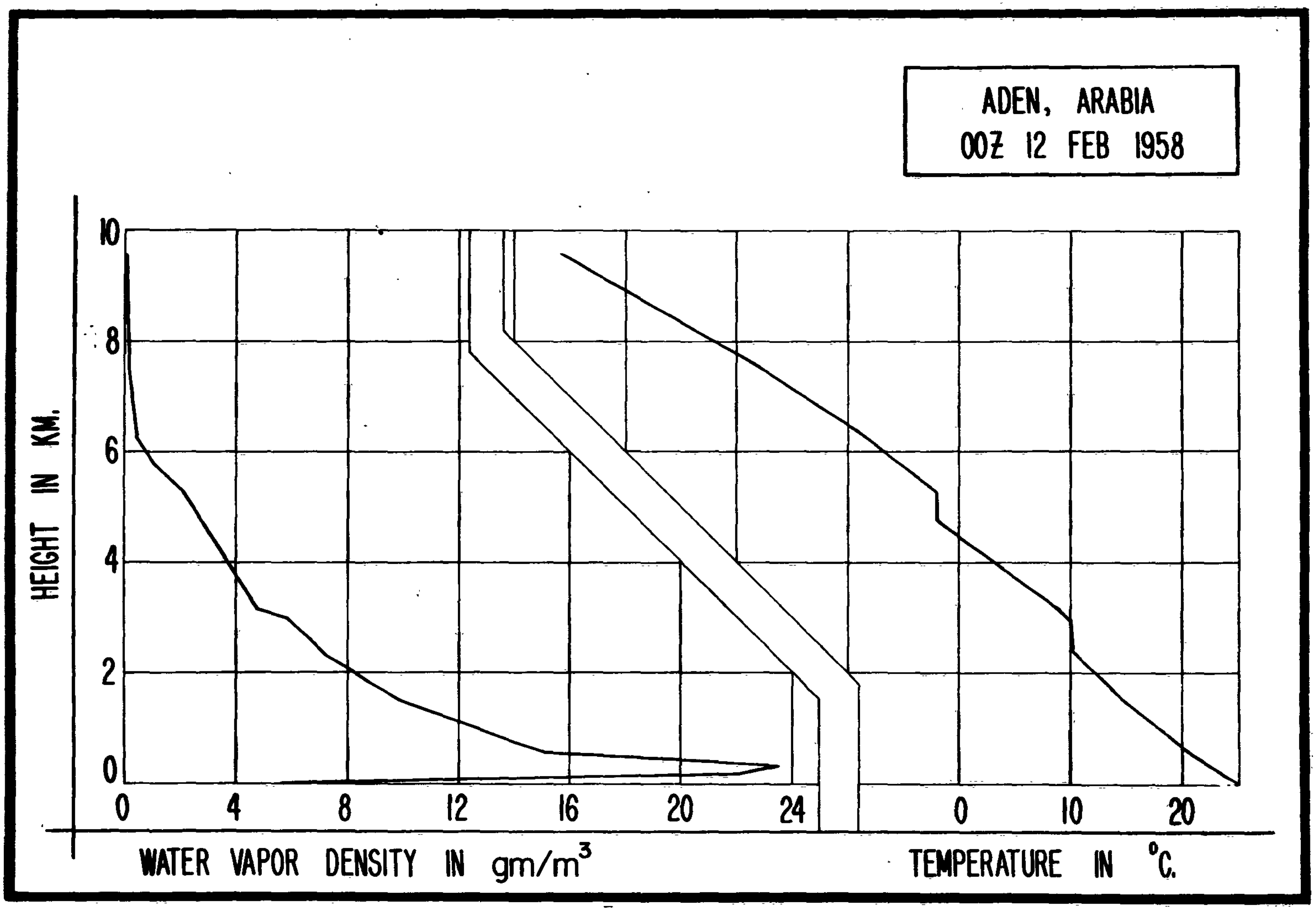

Fig. 17. Water vapor and temperature profile for Aden, Arabia.

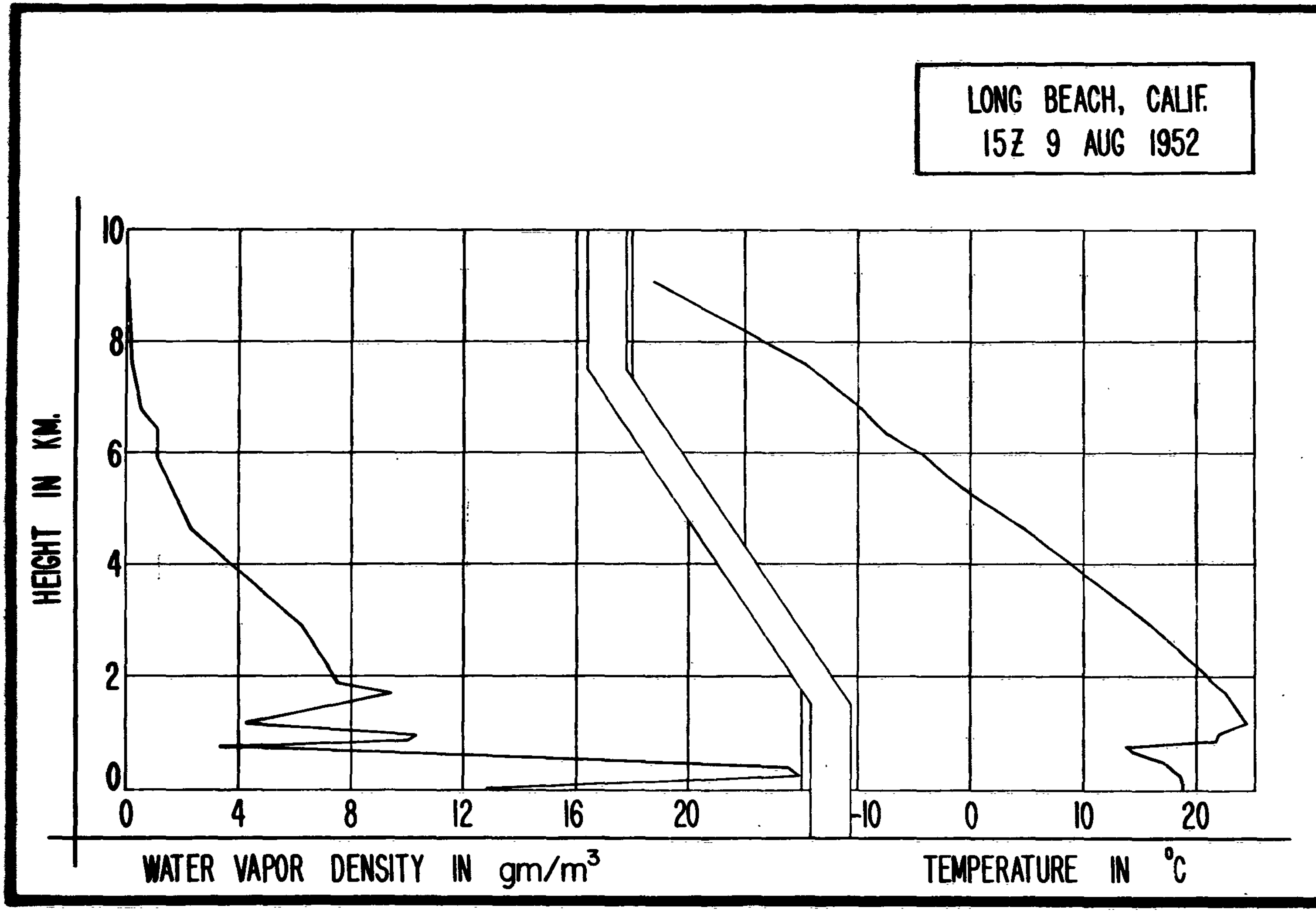

Fig. 18. Water vapor and temperature profile for Long Beach, California.

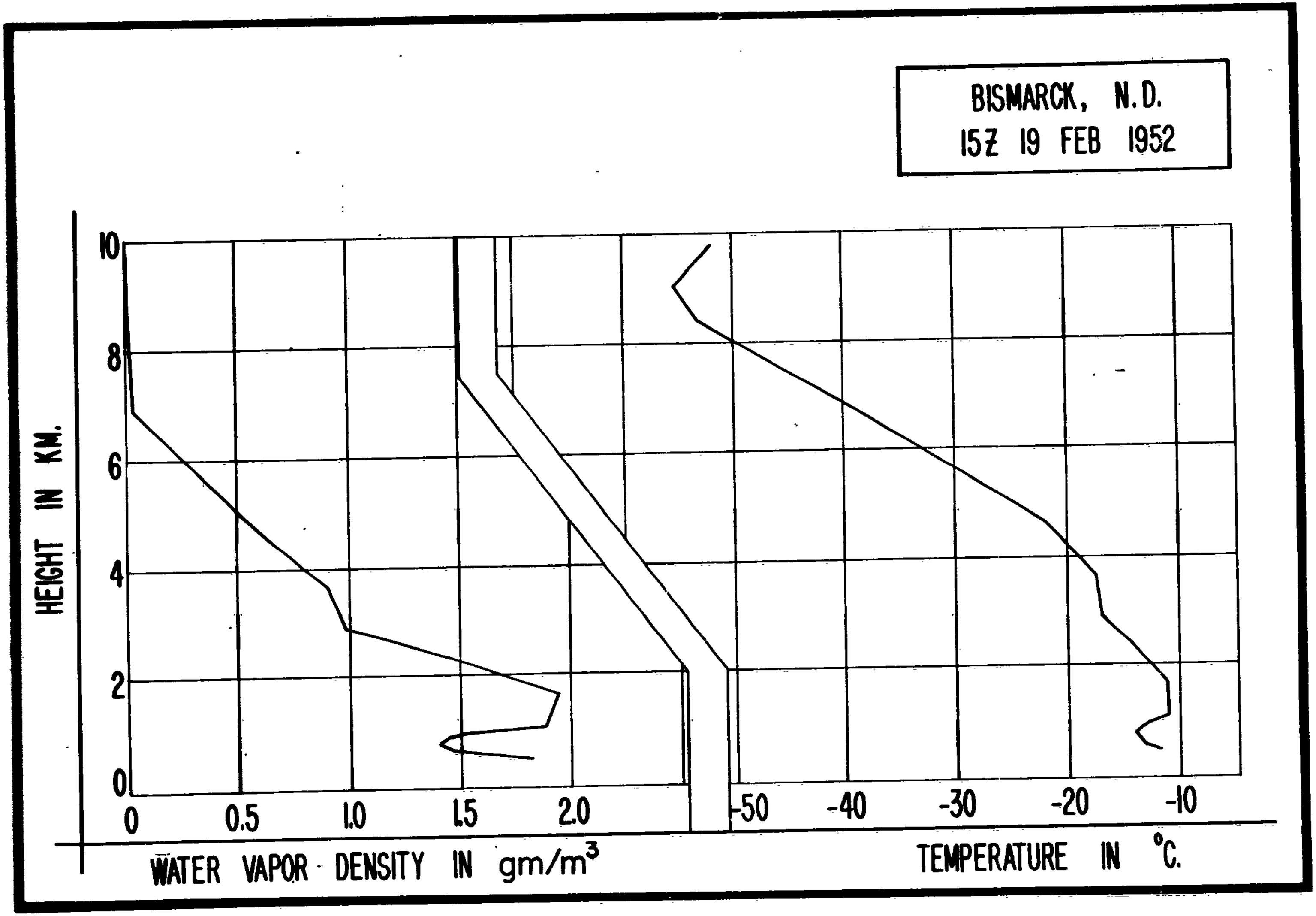

Fig. 19. Water vapor and temperature profile for Bismarck, N. Dakota.

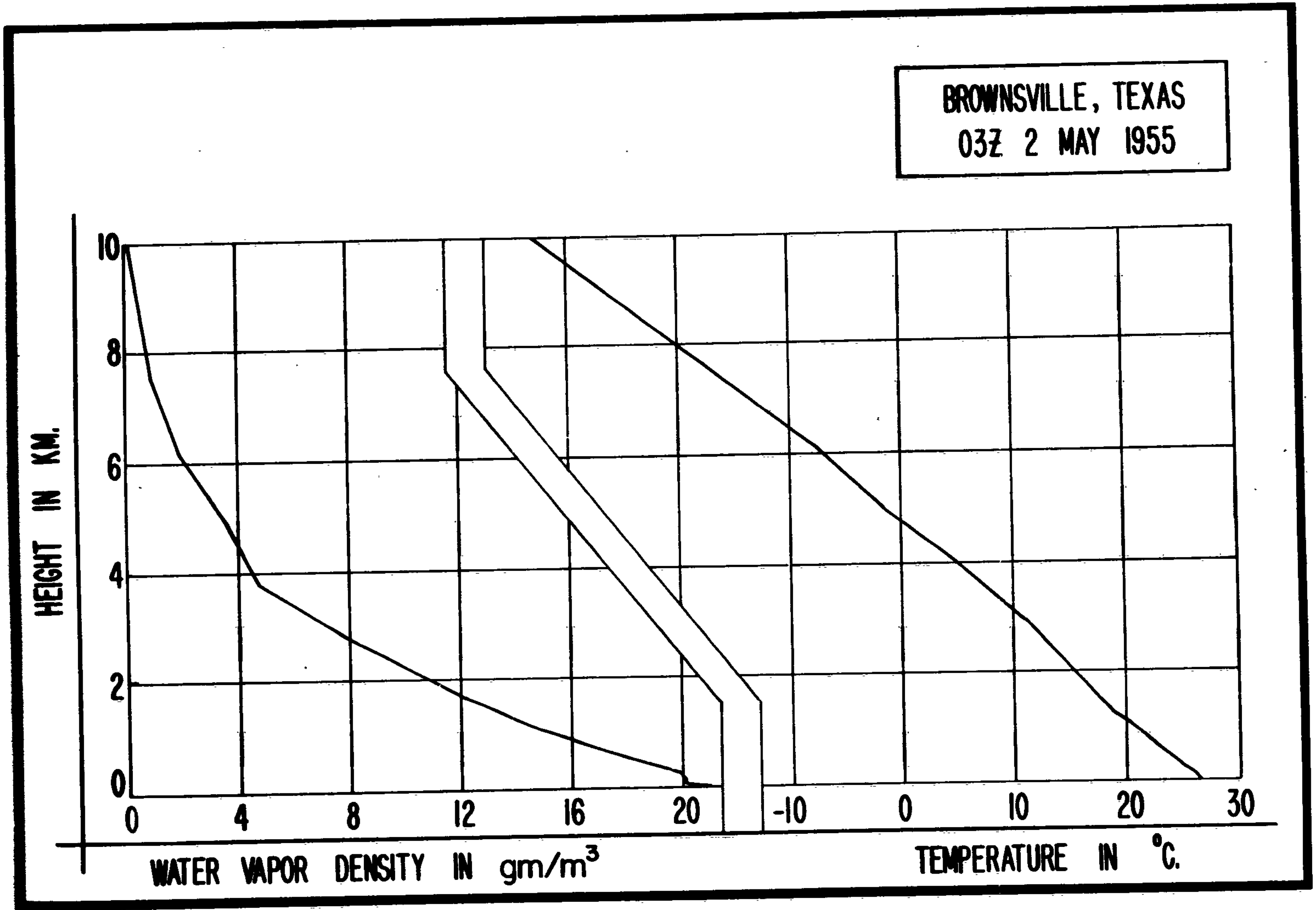

Fig. 20. Water vapor and temperature profile for Brownsville, Texas.

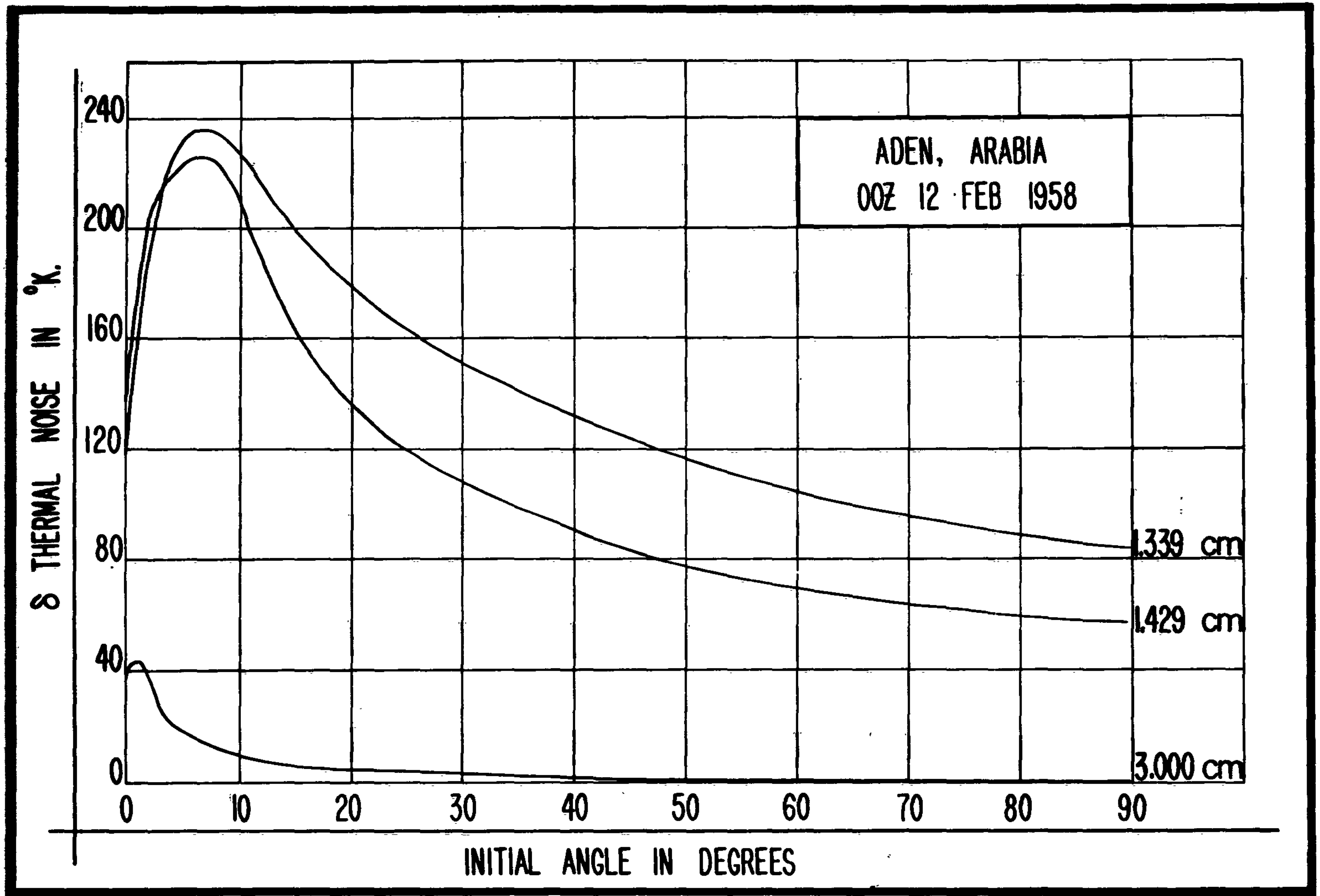

Fig. 21. Thermal noise departure from zero humidity standard atmosphere vs antenna elevation angle for Aden, Arabia.

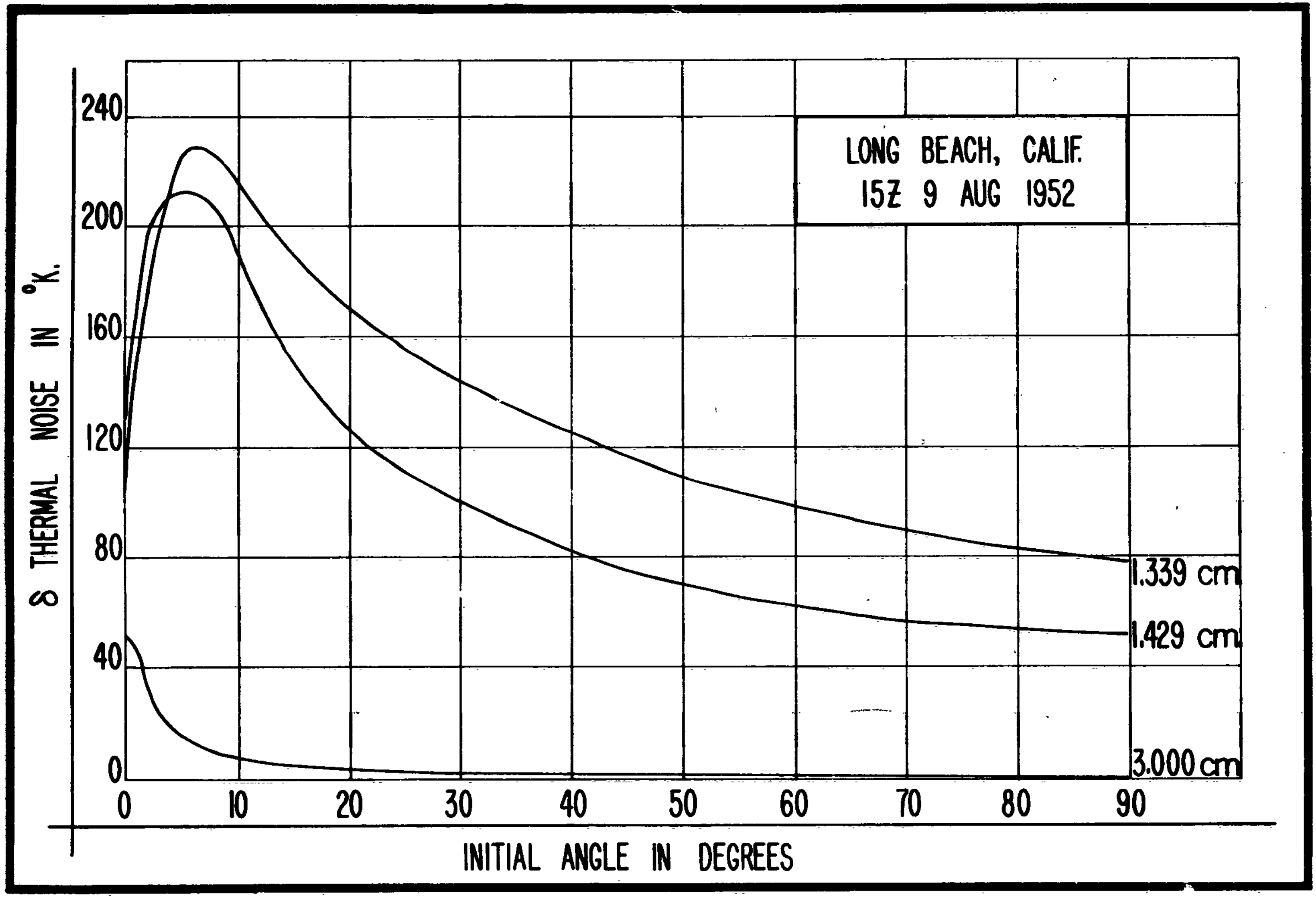

Fig. 22. Thermal noise departure from zero humidity standard atmosphere vs antenna elevation angle for Long Beach, California.

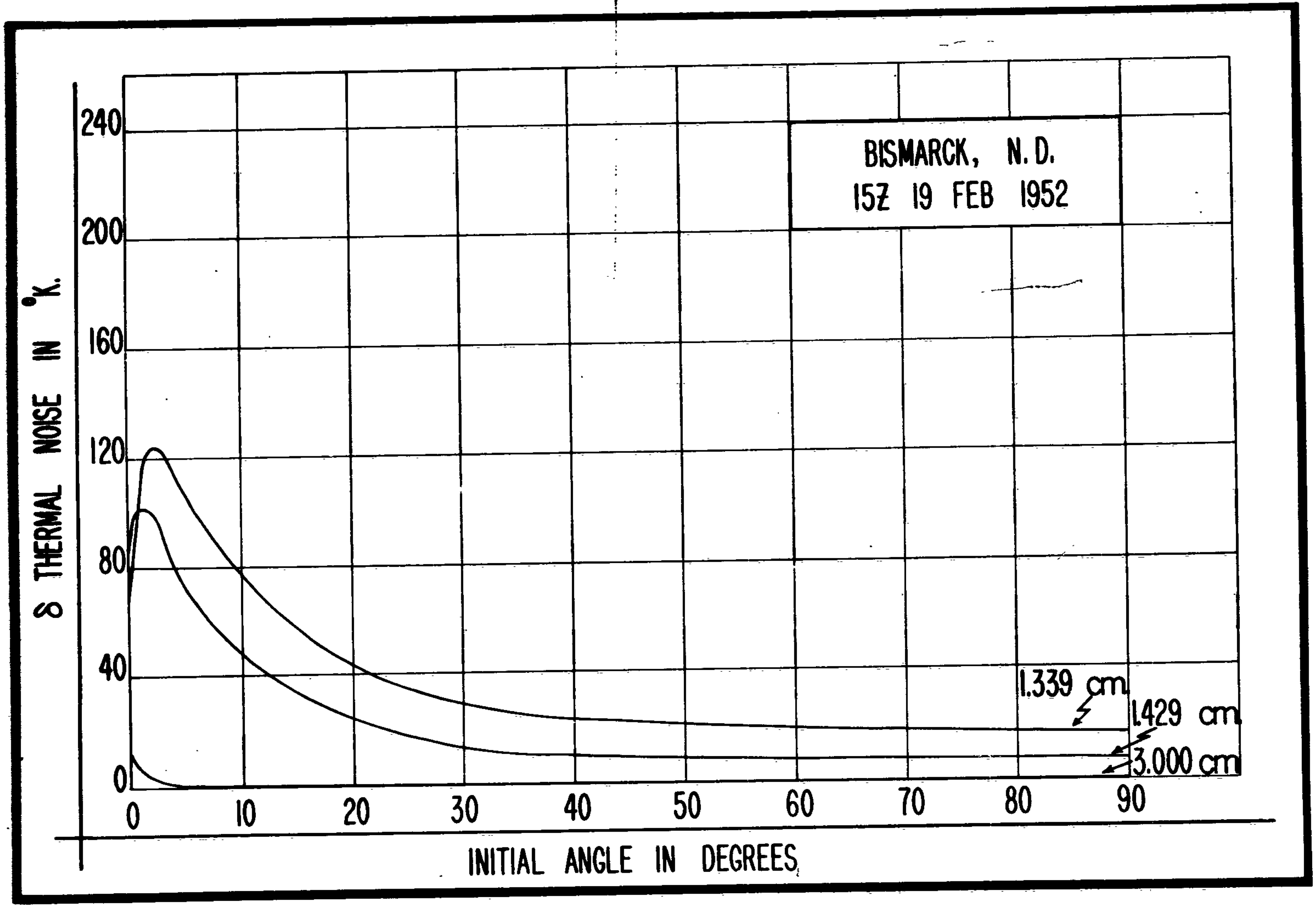

Fig. 23. Thermal noise departure from zero humidity standard atmosphere vs antenna elevation angle for Bismarck, N. Dakota.

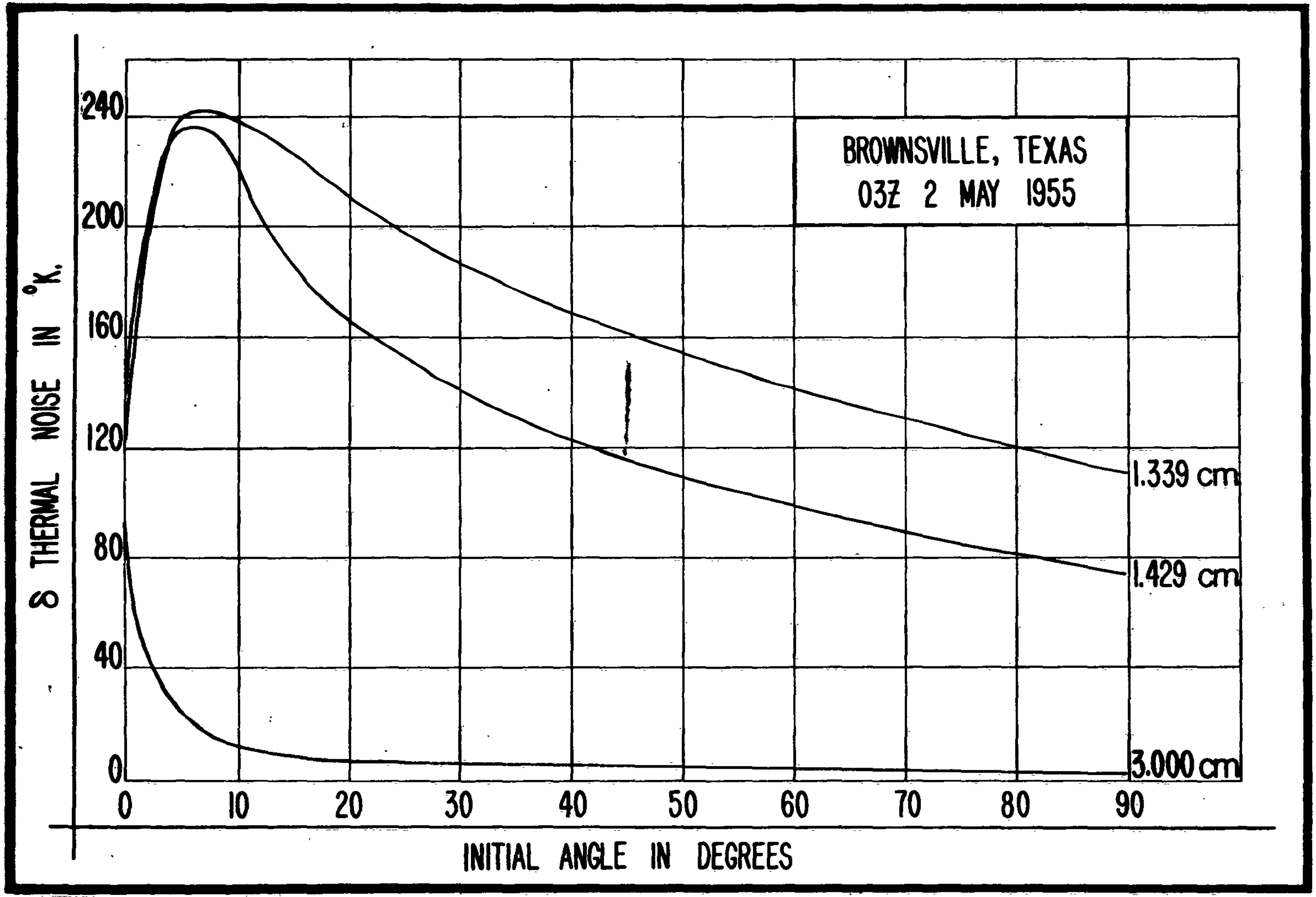

Fig. 24. Thermal noise departure from zero humidity standard atmosphere vs antenna elevation angle for Brownsville, Texas.

References

Artman, J. O., Absorption of microwaves by oxygen in the millimeter wavelength region, Columbia Radiation Laboratory Report, June, 1953.

Bean, B. R., and R. L. Abbott, Oxygen and water vapor absorption of radio waves in the atmosphere, Geofisica Pura e Applicata-Milano 37, 127-144 (1957).

Bean, B. R., and B. A. Cahoon, The use of surface weather observations to predict the total atmospheric bending of radio waves at small elevation angles, Proc. IRE 45, 1545-1546 (Nov. 1957).

Becker, G. E., and S. H. Autler, Water-vapor absorption of electromagnetic radiation in the centimetre wave-length range, Phys. Rev. 300 (1946).

Birnbaum, G., and A. A. Maryott, Microwave absorption in compressed oxygen, Phys. Rev. 99, 1886 (Sept. 1955).

Compendium of Meteorology (Waverly Press, Inc., Baltimore, Md. 1951).

Ghosh, S. N., and H. D. Edwards, Rotational frequencies and absorption coefficients of atmospheric gases, Air Force Surveys in Geophysics, No. 82 (1956).

Gunn, K. L. S., and T. W. R. East, The micro-wave properties of precipitation particles, Quart. J. Roy. Meteorological Soc., London XXX, 552-545 (1954).

Hill, R. M., and W. Gordy, Zeeman effect and line breadth studies of the microwave lines of oxygen, Phys. Rev. 93(5), 1019 (1954).

Planck, Max, The theory of heat radiation, (Dover Publications Inc., New York, 1959).

Ratner, B., Upper air average values of temperature, pressure, and relative humidity over the United States and Alaska, U. S. Weather Bureau (May, 1945).

Richtmyer, Kinnard, and Lauritsen, Introduction to Modern Physics, Chap. 4, (McGraw-Hill Book Co., New York, 1955).

Straiton, A. W., and C. W Tolbert, Anomalies in the absorption of radio waves by atmospheric gases, Proc. IRE 48, No. 5, 898-903 (1960).

Tinkham, M., and M. W. P. Strandberg, Line breadths in the microwave magnetic resonance spectrum of O_2, Phys. Rev. 99, 538 (1955).

Tolbert, C. W., and A. W. Straiton, Experimental measurement of the absorption of millimeter radio waves over extended ranges, Trans. IRE AP-5, No. 2, 239-241 (April 1957).

Van Vleck, J. H., Absorption of microwaves by oxygen, Phys. Rev. 71, 413-424 (April 1947a).

Van Vleck, J. H., The absorption of microwaves by uncondensed water vapor, Phys. Rev. 71, 421-433 (1947b).

Van Vleck, J. H., Theory of absorption by uncondensed gases, Propagation of Short Radio Waves, pp. 646-664 (McGraw-Hill Book Co., New York, 1951).

Weber, Eric, Apparent sky temperature in the microwave region, J. Meteorology 17, 159 (1960).

U. S. ARMY SIGNAL R&D LABORATORY
Fort Monmouth, New Jersey

SIGRA/SL-SMI 28 March 1962

CONTRACT REPORT DISTRIBUTION LIST
Distribution List for National Bureau of Standards
(MIPR R-61-3-SC-00-91)

	No. Copies
OASD (R&E), Rm 3E1065 ATTN: Technical Library The Pentagon Washington 25, D. C.	1
Chief of Research and Development OCS, Department of the Army Washington 25, D. C.	1
Chief Signal Officer ATTN: SIGRD Department of the Army Washington 25, D. C.	1
Chief Signal Officer ATTN: SIGOP-5 Department of the Army Washington 25, D. C.	1
Chief Signal Officer ATTN: SIGAC Department of the Army Washington 25, D. C.	1
Chief Signal Officer ATTN: SIGPL Department of the Army Washington 25, D. C.	1
Director U. S. Naval Research Laboratory, Code 2027 Washington 25, D. C.	1
Commanding Officer and Director U. S. Navy Electronics Laboratory San Diego 52, California	1
U. S. National Bureau of Standards Boulder Laboratories ATTN: Library Boulder, Colorado	1

	No. Copies
Commander Aeronautical Systems Division ATTN: ASAPRL Wright-Patterson Air Force Base, Ohio	1
Commander, Air Force Cambridge Research Laboratories ATTN: CRO L. G. Hanscom Field Bedford, Massachusetts	1
Commander, Air Force Command & Control Dev. Div. ATTN: CRZC L. G. Hanscom Field Bedford, Massachusetts	1
Commander, Air Force Command & Control Dev. Div. ATTN: CCRR& CCSD L. G. Hanscom Field Bedford, Massachusetts	2
Commander, Rome Air Development Center ATTN: RAALD Griffiss Air Force Base, New York	1
Commanding General U. S. Army Electronic Proving Ground ATTN: Technical Library Fort Huachuca, Arizona	1
Commander Armed Services Technical Information Agency ATTN: TIPCR, Arlington Hall Station Arlington 12, Virginia	10
Chief, U. S. Army Security Agency Arlington Hall Station Arlington 12, Virginia	2
Deputy President U. S. Army Security Agency Board Arlington Hall Station Arlington 12, Virginia	1
Commanding Officer U. S. Army Signal Equipment Support Agency ATTN: SIGMS-ADJ Fort Monmouth, New Jersey	1

	No. Copies
Corps of Engineers Liaison Office U. S. Army Signal R&D Laboratory Fort Monmouth, New Jersey	1
AFSC Liaison Office Naval Air R&D Activities Command Johnsville, Pennsylvania	1
Marine Corps Liaison Office U. S. Army Signal R&D Laboratory Fort Monmouth, New Jersey	1
Commanding Officer U. S. Army Signal R&D Laboratory ATTN: Director of Research Fort Monmouth, New Jersey	1
Commanding Officer U. S. Army Signal R&D Laboratory ATTN: Technical Documents Center Fort Monmouth, New Jersey	1
Commanding Officer U. S. Army Signal R&D Laboratory ATTN: File Unit #3 Fort Monmouth, New Jersey	1
Commanding Officer U. S. Army Signal R&D Laboratory ATTN: Technical Information Division Fort Monmouth, New Jersey	3
Commanding Officer U. S. Army Signal Missile Support Agency Missile Geophysics Division White Sands Missile Range, New Mexico	1
Director, Atmospheric Sciences Foundation National Science Foundation Washington 25, D. C.	1
The University of Texas Electrical Engineering Research Laboratory Austin, Texas	1
American Meteorological Society Abstracts and Bibliography P. O. Box 1736 Washington 13, D. C.	1

	No. Copies
New York University Meteorology Department University Heights New York 53, New York	1
Library U. S. Weather Bureau Washington 25, D. C.	1
Signal Corps Liaison Office, MIT 77 Massachusetts Avenue Bldg 26, Room 131 Cambridge 39, Massachusetts	1
Brookhaven National Laboratories Camp Upton, New York	1
Mr. Jack Pierrard Armour Research Foundation Chicago, Illinois	1
Mr. Harry Moses, Radiological Physics Division Argonne National Laboratory 9700 South Cass Avenue Argonne, Illinois	1
Dr. David Atlas Chief, Weather Radar Branch, GRD AFCRL Weather Radar Field Site Sudbury, Massachusetts	1
Transportation Officer for Activity Supply Officer U. S. Army Signal R&D Laboratory, Logistics Division Bldg 2504, Charles Wood Area Fort Monmouth, New Jersey Marked for: SIGRA/SL-SMI (MIPR R-61-3-SC-00-91)	14
Midwest Research Institute 425 Volker Boulevard Kansas City 10, Missouri Attention: Mr. R. W. Fetter	1

U. S. DEPARTMENT OF COMMERCE
Luther H. Hodges, *Secretary*

NATIONAL BUREAU OF STANDARDS
A. V. Astin, *Director*

THE NATIONAL BUREAU OF STANDARDS

The scope of activities of the National Bureau of Standards at its major laboratories in Washington, D.C., and Boulder, Colorado, is suggested in the following listing of the divisions and sections engaged in technical work. In general, each section carries out specialized research, development, and engineering in the field indicated by its title. A brief description of the activities, and of the resultant publications, appears on the inside of the front cover.

WASHINGTON, D. C.

Electricity. Resistance and Reactance. Electrochemistry. Electrical Instruments. Magnetic Measurements. Dielectrics. High Voltage.

Metrology. Photometry and Colorimetry. Refractometry. Photographic Research. Length. Engineering Metrology. Mass and Scale. Volumetry and Densimetry.

Heat. Temperature Physics. Heat Measurements. Cryogenic Physics. Equation of State. Statistical Physics.

Radiation Physics. X-ray. Radioactivity. Radiation Theory. High Energy Radiation. Radiological Equipment. Nucleonic Instrumentation. Neutron Physics.

Analytical and Inorganic Chemistry. Pure Substances. Spectrochemistry. Solution Chemistry. Standard Reference Materials. Applied Analytical Research. Crystal Chemistry.

Mechanics. Sound. Pressure and Vacuum. Fluid Mechanics. Engineering Mechanics. Rheology. Combustion Controls.

Polymers. Macromolecules: Synthesis and Structure. Polymer Chemistry. Polymer Physics. Polymer Characterization. Polymer Evaluation and Testing. Applied Polymer Standards and Research. Dental Research.

Metallurgy. Engineering Metallurgy. Microscopy and Diffraction. Metal Reactions. Metal Physics. Electrolysis and Metal Deposition.

Inorganic Solids. Engineering Ceramics. Glass. Solid State Chemistry. Crystal Growth. Physical Properties. Crystallography.

Building Research. Structural Engineering. Fire Research. Mechanical Systems. Organic Building Materials. Codes and Safety Standards. Heat Transfer. Inorganic Building Materials. Metallic Building Materials.

Applied Mathematics. Numerical Analysis. Computation. Statistical Engineering. Mathematical Physics. Operations Research.

Data Processing Systems. Components and Techniques. Computer Technology. Measurements Automation. Engineering Applications. Systems Analysis.

Atomic Physics. Spectroscopy. Infrared Spectroscopy. Far Ultraviolet Physics. Solid State Physics. Electron Physics. Atomic Physics. Plasma Spectroscopy.

Instrumentation. Engineering Electronics. Electron Devices. Electronic Instrumentation. Mechanical Instruments. Basic Instrumentation.

Physical Chemistry. Thermochemistry. Surface Chemistry. Organic Chemistry. Molecular Spectroscopy. Elementary Processes. Mass Spectrometry. Photochemistry and Radiation Chemistry.

Office of Weights and Measures.

BOULDER, COLO.

Cryogenic Engineering Laboratory. Cryogenic Equipment. Cryogenic Processes. Properties of Materials. Cryogenic Technical Services.

CENTRAL RADIO PROPAGATION LABORATORY

Ionosphere Research and Propagation. Low Frequency and Very Low Frequency Research. Ionosphere Research. Prediction Services. Sun-Earth Relationships. Field Engineering. Radio Warning Services. Vertical Soundings Research.

Radio Propagation Engineering. Data Reduction Instrumentation. Radio Noise. Tropospheric Measurements. Tropospheric Analysis. Propagation-Terrain Effects. Radio-Meteorology. Lower Atmosphere Physics.

Radio Systems. Applied Electromagnetic Theory. High Frequency and Very High Frequency Research. Frequency Utilization. Modulation Research. Antenna Research. Radiodetermination.

Upper Atmosphere and Space Physics. Upper Atmosphere and Plasma Physics. High Latitude Ionosphere Physics. Ionosphere and Exosphere Scatter. Airglow and Aurora. Ionospheric Radio Astronomy.

RADIO STANDARDS LABORATORY

Radio Physics. Radio Broadcast Service. Radio and Microwave Materials. Atomic Frequency and Time-Interval Standards. Radio Plasma. Millimeter-Wave Research.

Circuit Standards. High Frequency Electrical Standards. High Frequency Calibration Services. High Frequency Impedance Standards. Microwave Calibration Services. Microwave Circuit Standards. Low Frequency Calibration Services.